EUROPEAN ORGANIZATION FOR NUCLEAR RESEARCH

CERN-EP/98-183
16 November 1998

SHAPE COEXISTENCE IN THE LIGHT PO ISOTOPES

A. M. Oros[a‡], K. Heyde[a♯], C. De Coster[a], B. Decroix[a]
R. Wyss[b]
B.R. Barrett[a,c] and P. Navratil[c†]

[a] Institute for Theoretical Physics, Proeftuinstr. 86, B-9000 Gent, Belgium
[b] KTH Stockholm, Sweden
[c] Department of Physics, University of Arizona, Tucson, AZ, 85721 USA
‡ Permanent address: Institute for Nuclear Physics and Engineering, Bucharest-Magurele, Romania
♯ present address: EP-ISOLDE, CERN, CH-1211, Geneva 23, Switzerland
† On leave of absence from the Institute for Nuclear Physics, Academy of Sciences of the Czech Republic, 25068 Rež near Prague, Czech Republic

Abstract

The systematics of the even light Po isotopes (N$\leq$126) are studied in the framework of the Particle-Core Model. The strong perturbation of the systematics in the very light isotopes is interpreted as arising from the interaction between regular and intruder structures. Results of Potential Energy Surface (PES) calculations and predictions of the Pairing Vibration Model support this interpretation. The mixing between the regular and intruder structures is studied within the IBM-2 and in a simple two-state mixing picture. Matrix elements of the interaction and their spin-dependence are extracted. The 'reconstructed systematics' show the coexistence of a spherical structure, which varies little with the neutron number, with an intruder band, strongly lowered in energy as the neutron number approaches midshell. The crossing of the two configurations takes place over a few isotopes; the intruder band becomes the ground-state configuration in ^{192}Po.

(ISOLDE GENERAL)

(*Submitted for publication in Nuclear Physics A)*

1 Introduction

The shape coexistence phenomenon is rather well-established in the Pb region, as well as around a number of other shell closures, and has been reviewed recently [1]. Nevertheless, clear experimental evidence for the appearance and evolution of shape coexisting configurations around Z=82 is mainly limited to the Pb, Hg and Pt nuclei.

It has been predicted within a shell-model interpretation of intruder states [2] that the maximal energy lowering for an e.g. proton mp-mh configuration should take place at the neutron midshell, where the number of the valence particles is largest and the resulting total proton-neutron interaction energy is strongest. It is, therefore, important to follow the behavior of the intruder states down to and past midshell, which for the neutron shell N=82−126 corresponds to N=104.

While the even-even neutron deficient Pt isotopes have been studied down to neutron number N=90 [3, 4] and the Hg isotopes down to N=96 [5, 6], $\gamma-$spectroscopy experiments become increasingly difficult to perform on nuclei with larger proton number in the same neutron number range. The Pb nuclei have been studied in-beam down to N=102 [7, 8, 9, 10], the Po nuclei down to N=108 [11, 12] and the Rn nuclei down to N=112 [13, 14]. Many of the previous results are very recent and are due to a very intensive activity close to the limits of the current experimental techniques, which concentrates on the shape coexistence phenomenon in the Pb mass region.

In the light Hg and Pt isotopes, a weakly deformed oblate configuration (2 and 4 proton holes, respectively) coexists with a more strongly deformed prolate configuration having presumably a microscopic π(2p-4h) and π(2p-6h) structure, respectively. In the Hg isotopes, which maintain an oblate ground-state, the intruder band comes lowest in energy for N=104 and 102 and increases in energy again for the very light isotopes [5]. In the Pt isotopes, the prolate band drops abruptly in energy to become the ground-state band for N=186–178 and then increases abruptly in energy for $N < 178$. The yrast sequence of the lightest studied Hg and Pt isotopes seems to indicate a transition toward an anharmonic vibrator regime [5, 13]; for Z=80, $N < 100$, Potential Energy Surface calculations [15] predict indeed a close to spherical ground-state.

In the Pb isotopes, the intruder configuration coming down in energy toward midshell (starting from the N=126 shell closure) is supposed to have a mainly proton 2p-2h structure, or oblate deformation when using a deformed mean-field picture[15]. The stronger deformed bands identified in ^{188}Pb and ^{186}Pb [7, 8] and very recently in ^{190}Pb and ^{184}Pb [9, 10] correspond most probably with a proton 4p-4h character, or prolate deformation, and become the yrast band in ^{186}Pb.

An equivalence between particle-like and hole-like excitations, which is the idea behind the intruder spin (I-spin) symmetry, deduced within the framework of the Extended proton-neutron Interacting Boson Model (EIBM) [16, 17, 18, 19], will imply the existence of intruder configurations for the $Z > 82$ nuclei as well. Predictions for the structure of intruder bands in the very light Po and Rn nuclei, which will be due to π(np-2h) excitations across the closed shell, can be made [20] using the analogy with π(2p-nh) intruder bands in the Hg and Pt nuclei with the same neutron number.

Still, the status of the experimental data is closely reflected in the level of identification of the shape coexistence phenomenon and in the understanding of the mixing between

structures with different deformation in this mass region. In contrast to the situation in the comparatively well-studied Pt, Hg and Pb isotopes, the question as to whether or not intruder configurations are playing a role in the low-energy level scheme of the Po isotopes is still open [12, 21, 22, 23, 24].

We argue in this paper that the predictions of several models, corroborated with the trend in the experimental data, support the interpretation of the systematics of the light Po isotopes in terms of shape coexisting configurations.

We briefly review, in Section 2, the experimental information on the low energy level scheme of the Po isotopes. A study of their systematics in the framework of the Particle-Core Model (PCM) is presented in Section 3. Detailed comparison of the calculations with the experimental data is made for the Po nuclei in the mass range A=210–200; it is shown that the PCM cannot describe the transition from the two-particle-like regime seen in the heavier Po isotopes to the more collective structure observed in ^{192}Po.

The predictions of the Pairing Vibration Model for excited 0^+ states are tested against the experimental data in Section 4, and arguments are found for a 4p-2h structure of the 0^+_2 states. Using predictions of the Pairing Vibration Model for relative decay probabilities involved in the $\alpha-$decay process of the Po isotopes, and experimental hindrance factors measured in $\alpha-$decay experiments, information is extracted about the amount of mixing between the 0^+ 2p and 4p-2h configurations.

Deformed mean-field Potential Energy Surface (PES) calculations are presented in Section 5 and the energy of the predicted shape coexisting 0^+ configurations are compared to the experimental data. In ^{192}Po, the intruder configuration is predicted to become the ground-state. Using this result and the experimental data, a simple two-state mixing calculation, between the spherical states and the members of the intruder band with the same spin and parity, is performed in Section 6. The mixing matrix elements are extracted for each spin- and parity-value, together with the unperturbed energies of the spherical and deformed states. Mixing calculations are further performed within the framework of the proton-neutron Interacting Boson Model (also referred to as the IBM-2).

The arguments for the appearance of shape coexisting configurations in the light Po isotopes, and information about their mixing, are summarized in Section 7.

2 Systematics

The systematics of the Po isotopes in the mass range 192–210 are presented in Fig. 1. Only the yrast and yrare states of positive parity and spin J=0,2,4,6,8 and 10 have been included in the figure. While there is substantially more information on the level scheme of the heavier isotopes ($A > 200$) than shown in the figure [26], the yrast sequence up to spin 8^+ summarizes all the levels known in ^{192}Po [11, 12]. The systematics presented also exhaust most of the experimental information on the excitation spectra of $^{198-194}$Po. We will examine Fig. 1 in some detail, since it contains most of the experimental ingredients regarding the pros and cons involved in the two (co-)existing interpretations of the light Po isotopes (see, for example, Refs. [11, 12]).

Concerning electromagnetic properties, very little is known about the isotopes with $A <$ 200. For the decay of the states shown in Fig. 1, the only transition probability measured is

the B(E2;$8^+_1 \rightarrow 6^+_1$) in ^{198}Po [27]. The g-factor of the 8^+_1 state in ^{198}Po is also known [27] and is consistent with a $(\pi\ 1h_{9/2})^2$ structure. The interpretation of the light Po isotopes must, therefore, rely upon the energy systematics and additional information obtained in $\alpha-$decay measurements [25], which will be discussed later.

Two simple expectations related to the characteristic features of a nucleus with 84 protons and an open neutron shell are that: (i) the two-proton particle degrees of freedom will play an important role in the excitation spectrum; and that (ii) the interaction between these two protons and the valence neutrons will be responsible for collective aspects. The low-energy level scheme of the closed shell (N=126) nucleus ^{210}Po clearly fulfills expectation (i) and offers a classic example of a 'two-particle nucleus'. Most of the excited levels up to $E_x \sim 5$ MeV can be understood in terms of simple two-proton excitations in the orbitals of the shell above Z=82, namely $\pi 1h_{9/2}$, $\pi 2f_{7/2}$, $\pi 1i_{13/2}$, $\pi 3p_{3/2}$, $\pi 2f_{5/2}$ and $\pi 3p_{1/2}$ (see section 3).

One conspicuous feature, which appears immediately after leaving the neutron shell closure, is the strong lowering in energy of the first and second excited 2^+ states and also in a somewhat lesser extent of the 4^+ states. In contrast, the energies of the first excited 6^+ and 8^+ states remain constant and the two states are very close together, as expected from a two-particle spectrum with the particles in the $1h_{9/2}$ orbital. The variation or constancy of the excitation energy can be related to the change or constancy of structure, respectively. An important contribution from the neutron degrees of freedom can be expected to be responsible for the lowering in energy and change of structure of the $2^+_{1,2}$ and $4^+_{1,2}$ states, while for the low-lying 6^+_1 and 8^+_1 states this contribution is probably much smaller.

The further variation of the neutron number brings little change to the systematics down to mass A=200. Notably, the energy of the first 2^+ state remains constant within 20 keV. The energy of the first 6^+ and 8^+ states increases with decreasing mass and the states remain very close together. The one exception from this very smooth variation is the behavior of the 0^+_2 state, identified in β^+/EC decay experiments [25, 28]. This state drops in energy by 600 keV between ^{202}Po and ^{200}Po, becoming the second excited state in the latter nucleus. Another interesting point is that the decay pattern of the 2^+_2 state, as observed in Refs. [25, 28], is different from the one seen in the heavier isotopes; notably, the transition to the first excited 2^+ state has an E0 component.

It seems that ^{200}Po marks the end of a 'regular regime', which is replaced, starting with ^{198}Po, by an abrupt downsloping trend for nearly all the states, as seen from the systematics. The work by Maj et al. [27] established the existence of a discontinuity in the energy spacing of the first excited 6^+ and 8^+ states (which increases) and also in the value of the reduced transition probability B(E2;$8^+_1 \rightarrow 6^+_1$) (which decreases) in ^{198}Po, as compared to the corresponding values in the heavier Po isotopes. A lowering in the excitation energy of the first 2^+ and 4^+ states was also noticed. These effects were interpreted as due to an increase in the collectivity of the low-lying states, collectivity which 'reaches' the 6^+_1 state, while the 8^+_1 state still keeps its mainly two-particle character [27]. Subsequent work by Alber et al. [29] revealed that the drop in the energy of the 6^+_1 state becomes much more pronounced in ^{196}Po and the 2^+_1 and 4^+_1 states are further lowered, while the energy of the 8^+_1 state follows the upsloping trend noticed in the heavier isotopes. Second excited 2^+ and 4^+ states were found in ^{198}Po and ^{196}Po, and the study of their decay to the first 2^+ and 4^+ states, respectively, gave indication of a quite strong E0 component [29]. Following this observation and its corroboration with predictions of Potential Energy Surface calculations, Alber et al.

interpreted the 2_2^+ and 4_2^+ states as being members of an expected collective band built on a deformed configuration. Mixing of this band with the ground-state quasiband could then be responsible for the observed perturbation in the systematics and also for E0 components in the decay of the mainly deformed to the mainly spherical states. A new, in-beam study of ^{196}Po and ^{198}Po, by Bernstein et al. [21], extended the information about the two nuclei and confirmed most of the previous results, but found no evidence for E0 components in the decay of the yrare 2^+ and 4^+ states. In none of the two experiments [29, 21] conversion electrons were actually measured and the evidence or lack thereof for the E0 component was obtained from missing- or fully observed $\gamma-$ray intensity, respectively. Bernstein et al. [21] offer an alternative explanation of the light Po isotopes to the one given by Alber et al. Using the branching ratios for the $\gamma-$decay of the 2_2^+ and 4_2^+ states in ^{198}Po and ^{196}Po, Bernstein et al. made a comparison using vibrational, rotational and "4p-2h" pictures and found that the experimental data seem to agree best to the vibrational limit. The ratios of different transition probabilities, to be compared to different predictions, were extracted from the experimental branching ratios under the assumption that the transitions involved have all pure E2 character. The energy ratios R($8^+/6^+$), R($6^+/4^+$), R($4^+/2^+$), seem to point to an evolution toward a vibrational regime, too. The cause for the increasingly collective vibrational character with decreasing neutron number was explained [21] as due to the increasing role of the $\nu i_{13/2}$ orbital and its larger overlap with the active orbital for the protons, $\pi h_{9/2}$.

The next nucleus, ^{194}Po, added to the systematics by the work of Younes et al. [22], showed that the 'dropping' trend continues for the yrast 2^+- 6^+ states and also reaches the 8^+ and 10^+ states. Yrare (2^+) and (4^+) states have been observed too. The spin assignments for all the states were based on systematics, since an angular correlations study was not allowed by the poor statistics. Based on energy ratios, it was noticed that the energy spectrum of ^{194}Po corresponds to that of an anharmonic vibrator, while the same ratios show ^{196}Po and ^{198}Po to be nearly harmonic [21]. This was interpreted as a possible rapid transition toward a deformed rotor, which, if the trend were to continue, could already take place in ^{192}Po.

The recent experiments by Helariuta et al. [11] and Fotiades et al. [12] provided information on excited states in ^{192}Po, which is the lightest Po isotope studied by $\gamma-$spectroscopy, and very close to the last Po isotope known to exist, ^{190}Po [30]. Although the energies of all the yrast levels continue to decrease, the energy ratios of the type R(E(J+2)/E(J)), with J$\geq$2, were found to be still far from what would be expected for a rigid rotor [12]. Fotiades et al. [12] further discuss the collective aspects met in the light Po isotopes down to mass number A=192 in the framework of the Particle-Core Model (PCM), making use of results obtained by Cizewski and Younes [23] and Younes and Cizewski [24]. It is concluded that the model can reproduce the experimental trend of the yrast levels, together with the yrare 2^+ and 4^+ states, via an increase in the particle-vibration coupling. The second excited 0^+ states, which were identified in the light Po isotopes down to A=196, from β^+/EC and $\alpha-$decay studies [25, 28], are nonetheless not reproduced by the model.

The alternative interpretation is heavily based on the observed low-lying 0_2^+ states, which are discussed in terms of intruder configuration [25, 11]. The perturbation in the systematics below A=200 is described qualitatively as being due to the mixing of the associated intruder band with the regular structures.

We performed a new and complete study of the N$\leq$126 Po nuclei in the framework of the Particle-Core Model [31], which demonstrates the need to include mixing with the

intruder configurations in order to describe correctly the evolution from the the two-particle-like regime seen in the heavier Po isotopes to the more collective structure observed in ^{192}Po.

3 A Particle-Core Model study of the Po isotopes

As noticed from the experimental data discussed in the previous section, the spectra of the Z=84 Po nuclei display features resulting from the combined effect of the two-proton degrees of freedom and the more collective neutron contribution.

It is possible to describe both aspects in the framework of the Particle-Core Model (PCM; also referred to as the Unified Model), when some natural truncations are imposed on the neutron as well as on the proton system. The role played by the neutron degrees of freedom in a given Po isotope can be first studied in the low-energy excitation spectrum of the Pb nucleus with the same neutron number, since proton excitations accross the Z=82 closed shell should become active at higher energies. We will limit the neutron configuration space to surface vibrations of quadrupole and octupole character. We discuss briefly, in sec. 3.2.2, the accuracy of this approximation of the neutron excitation spectrum. For the proton degrees of freedom, excitations involving the orbitals of one major shell (in this case Z=82-126) have been considered. Their characteristics can be best studied in the odd-mass Bi isotopes, taking into account the coupling of the one-proton degrees of freedom to neutron collective excitations. In the calculations performed on the odd-mass Bi isotopes, an extra type of proton excitations, π(2p-1h), have been taken into account, with the hole orbital belonging to the Z=50–82 major shell. We mention that the intruder excitations, which involve the breaking of the closed proton core, are well taken into account for the Bi isotopes as being of (spherical) 2p-1h character, but not for the Po nuclei, where they would be of 4p-2h character.

3.1 The model

We will not insist on the details of the Particle-Core Model, since the formalism and its application to a large number of even-even and odd-mass nuclei are available in extensive literature (see for example [31, 32, 33, 34, 35, 36, 37, 38]). Instead, we only mention here the main features of the model, for consistency. The basis consists of collective$\otimes$single-particle or two-particle wave-functions. For the collective part, a multiphonon spectrum is considered, built up of quadrupole and octupole phonons. Anharmonic effects are accounted for by taking into account the quadrupole moments of the quadrupole and octupole phonons. This removes the degeneracy of multiphonon multiplets, via the quadrupole-quadrupole interaction and also accounts for the observed splitting of the particle-vibration multiplets. For the single-particle excitations, one major shell is usually considered; in the case of odd nuclei, where 2p-1h excitations are also taken into account, two major shells are considered. We use the single-particle wave-functions given by the harmonic oscillator potential. The single-particle energies are allowed to vary and are determined from comparison of the model calculations with the experimental data, as will be discussed in section 3.2. For calculations on the even-even nuclei, the two-particle spectrum and wave-functions are obtained from the single-particle hamiltonian described above and a Surface Delta Interaction (SDI). The hamiltonian

is given by:

$$H = \sum_{i=1,2} \sum_{j} h_{\rm sp}^{(i)}(j) + H_{\rm SDI}(1,2) + H_{\rm PVC}, \tag{1}$$

with

$$h_{\rm sp}(j) = \epsilon_j \, a_j^\dagger \cdot \tilde{a}_j, \qquad H_{\rm SDI}(1,2) = G\,\delta(\vec{r}_1 - \vec{r}_2)\delta(r_1 - R_0), \qquad \text{and}$$

$$\mathrm{H_{PVC}} = -\sum_{i=1,2} \sum_{\lambda=2,3} \xi_\lambda \hbar\omega_\lambda (\tfrac{\pi}{2\lambda+1})^{1/2} \tfrac{r^\lambda}{<r^\lambda>} \sum_{\mu=-\lambda}^{\lambda} [b_{\lambda\mu}^\dagger + (-)^\mu b_{\lambda-\mu}] Y_{\lambda\mu}^*(i), \tag{2}$$

where ϵ_j is the single-particle energy of a given orbital (nlj), G is the strength of the SDI, ξ_λ is the strength of the particle-vibration coupling of multipole λ, $\hbar\omega_\lambda$ is the energy of the vibrational 2^λ-pole phonon in the core Pb nucleus, $< r^\lambda >$ is the mean value of the radial integral for the orbitals in the major shell, and $a_j^\dagger$, $\tilde{a}_j$ and $b_{\lambda\mu}^\dagger$, $b_{\lambda-\mu}$ are the creation and annihilation operators for the fermionic (single-particle) and bosonic (collective phonons) excitations, respectively.

The parameters of the model are thus the two strengths of the particle-vibration coupling, ξ_2 and ξ_3 for the quadrupole and octupole term, respectively, the strength of the Surface Delta Interaction, G, the quadrupole moments of the quadrupole and octupole phonons, $\mathrm{Q}(2^+)$ and $\mathrm{Q}(3^-)$, respectively, and the single-particle energies. Additionally, in calculations on the even-even nuclei, the energies of the quadrupole and octupole phonons are allowed to differ somewhat (10–20%) from the experimental energies of the 2_1^+ and 3_1^- states of the core, in order to account for polarization effects due to the two extra nucleons.

3.2 Parameters and fitting procedure

In order to fix most of the model parameters used in the calculations for the Po isotopes in an unambiguous way, we have performed simultaneously a study of the odd-proton Bi isotopes with the corresponding neutron numbers. Thus the strengths of the particle-vibration coupling, the quadrupole moments of the vibrational phonons and the proton single-particle energies were fixed from comparison between the calculations and the experimental data in the Bi isotopes, and subsequently used for the calculations performed on the Po isotopes as well.

3.2.1 Bi isotopes

The experimental information needed to fix the parameters of the Particle-Core Model concerns level energies, electromagnetic properties and spectroscopic factors for a number of levels with collective or single-particle components. While it is important to have relevant experimental information concerning the dominant structure of certain levels, as, for example, collective components from inelastic scattering of charged particles or Coulomb excitation, and single-particle components from one-particle transfer reactions, the study of a whole isotopic chain facilitates the extrapolation of the parameters from well-studied nuclei to nuclei where only reduced information is available.

The only stable Bi isotope is ^{209}Bi, where a classic example of a particle-octupole vibration multiplet has been identified by inelastic scattering and Coulomb excitation experiments (see

e.g. [39] for a discussion). Regarding information on the single-particle character of states in this isotopic chain, as obtained in one-nucleon transfer reactions, this is only available down to ^{205}Bi, below which the required Pb targets become unstable.

The levels needed to estimate the strength of the particle-vibration coupling and (some of) the single-particle energies are experimentally known in the Bi isotopes down to ^{199}Bi. For the lighter nuclei, one has to extrapolate the values by assuming that their evolution is smooth.

The odd-mass Bi isotopes are reproduced quite satisfactorily by the model. In figure 2, the experimental information concerning energies and spectroscopic factors of relevant levels is compared to the results of the calculations for the isotopes ^{209}Bi, ^{207}Bi and ^{205}Bi.

3.2.2 Pb cores

In the Particle-Core Model calculations on the Bi and Po isotopes, the Pb cores are described as anharmonic vibrators. The particle-vibration coupling strengths can be determined from the B(E2) and B(E3) reduced transition probabilities for the decay of the 2_1^+ and 3_1^- "phonon"-states to the ground-state. No such values are known below ^{204}Pb. The available B(E2)-values [26] show an abrupt drop from the p-h excitation in ^{208}Pb to the two neutron-hole state of ^{206}Pb, followed by an increase when going to the four neutron-hole nucleus ^{204}Pb. The B(E3) values are constant within the error bars for $^{208-204}$Pb [26], and the excitation energy of the 3_1^- state varies very little. In ^{202}Pb, the first 3^- is 100 keV lower than in ^{204}Pb, but no B(E3)-value is available. No excited 3^- states are known in ^{200}Pb and ^{198}Pb and below ^{196}Pb. Nevertheless, the drop in the energy of the 3_1^- state by more than 500 keV between ^{202}Pb and ^{196}Pb suggests an increase in the octupole collectivity over this mass region.

A description of the Pb isotopes in terms of anharmonic vibrators clearly leaves out of the configuration space most of the neutron excitations, mainly of two quasi-particle (2qp) character, as well as specific proton excitations across the Z=82 shell gap (of 2p-2h, 4p-4h, ..., character). The effect of the (2qp) core excitations not taken into account by the model on the predicted excitation spectra of the odd-mass, core+1 nuclei, was investigated in a study of the collective and non-collective excitations in the N=83 nuclei [33]. The influence of the (proton)2qp$\otimes$neutron configurations on the energies and spectroscopic factors of the states with single-particle and collective $\otimes$ single-particle structure was found to be very reduced. In other words, the two subspaces, one including only 2qp excitations of the core, coupled to single-particle excitations, the other including only collective $\otimes$ single-particle states (the normal configuration space of the Particle-Core Model), are nearly orthogonal. The effects are large only when configurations belonging to the two subspaces are nearly degenerate. The effects of the same configurations on the excitation spectra of the N=84 nuclei (with application to ^{146}Sm) were studied phenomenologically in Ref. [37], with very similar conclusions. The states corresponding to the core 2qp states $\otimes$ two neutrons (in the case of N=84 nuclei) were found to lie at energies very close to the energies of the 2qp states, as seen in the core, plus the energy of the two-neutron states, taken from the low-lying spectrum of the N=84 nuclei. The same results hold for the Bi and Po nuclei, concerning neutron 2qp excitations coupled to proton one- or two-particle states.

Therefore, one expects that a number of states seen in the Bi and Po isotopes cannot be

reproduced by calculations in the framework of the Particle-Core Model. As can be seen from the quality of our results for the Bi isotopes shown in Fig. 2, the effect of neutron 2qp $\otimes$ one proton configurations on the states of interest is very reduced. Our calculations for the Po isotopes concentrate on the yrast and yrare states up to a moderate spin (J$\leq$10) and mainly of positive parity. For such energies and spins, the core 2qp configurations which are outside the model space are expected to play a role only when coupled to the lowest two-proton state, $(\pi^2)0^+$.

We illustrate this point in Fig. 3, where the excitation spectrum predicted in the harmonic vibrator picture, starting from quadrupole surface vibrations, is compared to the experimental spectrum for ^{206}Pb and ^{204}Pb. The experimental data include only states up to an excitation energy of 2 MeV, with positive parity and spin values in the interval J=0–4. Some of the states were interpreted as 2qp states in Ref. [40]. The data are taken from Ref. [26]. The states with ν(2qp) structure give rise to corresponding excitations in the Po isotopes, when coupled to a pair of protons, and will result in states with the same spin and parity and at similar energies as in the core.

In the light Pb isotopes starting with (and lighter than) ^{198}Pb, the first excited 0^+ state lies below 1.5 MeV excitation energy [41]. Its energy decreases rapidly with decreasing neutron number, and it even becomes the first excited state in $^{190-194}$Pb. Furthermore, a systematic lowering of the energy of the first excited 2^+ state was observed below ^{198}Pb. The low-lying 0_2^+ states were interpreted in Ref. [41] as corresponding to a deformed proton two-particle two-hole excitation. The mixing of the deformed 0_2^+ state and its associated band (only up to spin 2^+) with the spherical structures of corresponding spin and parity was studied in Ref. [42]. As a result of the study, it was shown that the 2_1^+ state changes character, from spherical in ^{198}Pb to a mainly deformed configuration in ^{190}Pb. After correcting for the mixing of the spherical and deformed 2^+ configurations, the unperturbed spherical configuration was found to remain at constant excitation energy in the isotopes below ^{198}Pb as well.

These results concerning the light Pb isotopes have an important impact on the interpretation of the Po isotopes in the Particle-Core Model. The 2^+ "phonon-state" of the Pb cores, as considered in the model basis, corresponds to the unperturbed spherical 2^+ configuration, and not anymore to the experimental first excited 2^+ state. The energy of the phonon 2^+ state should therefore remain basically constant in the calculations which involve Pb cores lighter than ^{198}Pb (corresponding to Po isotopes lighter than ^{200}Po). Associated with the constant energy, no important increase in the quadrupole strength of the particle-vibration coupling is expected. This is a clear physical restriction to the range of variation of the model parameters. It is even more important since it refers to the mass range where not enough data are available in the Bi isotopes to allow a clear determination of the PCM parameters.

The Particle-Core model in the way used here for the even Po isotopes does not take into account excitations which involve the breaking of the closed proton core, as are the proton two-particle two-hole excitations. The question of where the corresponding proton four-particle two-hole excitations are to be found in the Po isotopes and what effect they have on the spherical spectrum cannot be answered in the framework of the model in its present form. This problem will be treated in the sections 4 and 6.

3.3 Results

The model reproduces well the known levels of the Po isotopes in the mass range A=210–200, as can be seen from the examples given in Figure 4. The Surface Delta Interaction clearly gives a good description of the excited levels of ^{210}Po, where the effect of the particle-vibration coupling is very reduced.

In contrast, the particle-vibration coupling plays a determining role in the low-energy excitation spectrum of the Po nuclei with an open neutron shell. As an example, the calculated first two 2^+ states are a nearly equal mixture of $(\pi^2)2^+$ and $2^+(\text{core})\otimes(\pi^2)0^+$ configurations.

Some of the low-lying states, which are not reproduced by the model, most probably involve neutron two-quasiparticle excitations in the open neutron shell, as discussed in subsection 3.2.2. As an example, for the $4^+_{1,3}$ states in ^{206}Po, states with the same spin and parity and very similar energy can be found in the corresponding ^{204}Pb core (see Fig. 3). The occasional not so good agreement between the calculated and experimental 2^+_2 states is probably due to the existence of excited 2^+_2 states in the Pb cores, which are outside the configuration space of the model. Even more convincing is the case of the low-lying negative-parity states with spin 5^-, 7^- and 9^- (not shown in Fig. 4), which lie significantly lower than possible two-proton states with that spin and parity (predicted around 3 MeV). As already observed before [27], the states are found at nearly the same excitation energy and have the same spin-parity as the low-lying negative-parity states of the Pb cores. The two facts together make the identification of the states as neutron excitations quite straightforward. The only experimentally known negative parity state to which a proton structure can be assigned is the 11^-_1 isomeric state. Its PCM wave function has a main $\pi(1\text{h}_{9/2}1\text{i}_{13/2})$ component in all the Po isotopes with N<126, but also a non-negligible ($\sim 25\%$) $2^+(\text{core})\otimes\pi(1\text{h}_{9/2}1\text{i}_{13/2})$ admixture. The slight disagreement between the calculated and experimental energy of the 11^-_1 state, as shown in figure 4, is probably due to the reduced number of model configurations leading to this rather high spin, which results in some basis truncation effects. A slightly lower single-particle energy for the $\pi 1\text{i}_{13/2}$ orbital will improve the agreement for the 11^- states. Nevertheless, we preferred to fix the single-particle energies to the values determined for the Bi isotopes, in order to reduce the number of free parameters used for the calculations on the Po isotopes.

The parameters used for the PCM calculations on $^{210-200}$Po are summarized in Table 1. To be noted is the only moderate increase in the quadrupole particle-vibration coupling strength, ξ_2, with decreasing mass. This is not a pronounced effect and, besides the expected weak coupling case met in ^{210}Po, the values of the parameters indicate intermediate coupling for the whole mass range studied. Another interesting feature of the parameters is the very reduced effect of the two extra protons on the energy of the phonon 2^+ state of the core. The values of the phonon energy, $\hbar\omega_2$, used in the calculations, corresponds within 50 keV to the experimental energy of the first excited 2^+ state, $\text{E}(2^+_1)$. As to the octupole coupling strength and phonon energy, some difficulties did arise from the scarceness of experimental information, in the Pb nuclei (see subsection 3.2.2) as well as in the Po isotopes. The first excited 3^- state is only known in ^{210}Po; for the other Po isotopes, the polarization effect on the energy of the octupole phonon state due to the two extra protons was estimated from the value found in ^{210}Po. For the coupling strength ξ_3, the relation $\hbar\omega_3 \cdot \xi_3 \sim$constant was used.

Due to the lack of relevant experimental data, one has to extrapolate nearly all the model parameters below A$\simeq$200. This is also the mass region where the pronounced perturbation of the systematics appears. A smooth extrapolation of the values of the parameters starting from the ones used for the heavier isotopes will only lead to a smooth evolution of the calculated energies and wave functions, in contradiction with the experimental picture. Before making any assumptions about how the parameters should behave for calculations on the Po nuclei below ^{200}Po, one should answer the question if, by any means, the model can describe the evolution of the light Po isotopes down to ^{192}Po.

Fig. 5 presents the evolution of the yrast line as a function of the main model parameters. Probably a very low value chosen for $\hbar\omega_2$, of around 350 keV, will give a reasonable fit to the energy of the levels known in ^{192}Po. Nevertheless, as pointed out in the previous subsection, this is by no means a physically acceptable solution. The energy of the 2^+ "phonon state" in the Pb cores lies at around 1.1 MeV for the whole range of light nuclei, as seen in Fig. 5 part d).

It is therefore clearly seen that the experimental yrast line of ^{192}Po - as well as the evolution towards it - cannot be described in the framework of the Particle-Core model, at least not when the constraint of keeping the parameters in a physically meaningful range is enforced.

This conclusion is contrary to the one reached in a previous Particle-Core study of the light Po isotopes [12, 23, 24]. The main difference probably arises from the different configuration spaces and the very different range of parameters used. The coupling of two protons moving in the $1h_{9/2}$ orbital only, to the vibrational core was taken into account in Ref. [24], while we used in this study all the orbitals of the whole major shell Z=82–126. It is most clearly seen that excitations involving all the orbitals have to be taken into account from the study of the experimental levels of ^{210}Po. The best coupling strengths found in the study of Ref. [24] for the Po isotopes heavier than ^{200}Po have the value zero. This means that the particle-vibration coupling has no influence on the Po isotopes above mass 200, quite in contrast with the results of the present study of the Po and Bi isotopes. A study of the quadrupole moments of the 8_1^+ states in the Po isotopes with mass number A=200-210 [43] also found evidence for non-negligible effects of the particle-vibration coupling in this mass region and enforces our conclusions. Furthermore, the value used in Ref. [24] for the energy of the quadrupole phonon amounted to $\sim$620 keV for all the isotopes below ^{210}Po (for which calculations were not performed). No octupole phonons were considered. The abrupt change in the systematics was reproduced in Ref. [24] by a steep change in the coupling parameters at mass 200. However, in the Particle-Core Model, which implies a clear distinction between the two-particle and the collective degrees of freedom, such an abrupt increase in the particle-vibration coupling should be correlated with an abrupt increase of collectivity in the core nuclei (and a corresponding decrease of the excitation energy of the phonon states). This does not seem to be the case in the Pb isotopes (see for example the discussion of Ref. [42]), where the decrease in the energy of the first excited 2^+ state is associated to the strong lowering in energy of an intruder configuration.

As a conclusion to this section, our study of the Po isotopes in the mass range A=200–210 shows a quite satisfactory agreement between the experimental level properties and the PCM calculations. It was also shown that the Particle-Core Model, used with physically meaningful parameters, is not able to reproduce the change of properties in the isotopes below ^{200}Po,

leading to the experimental spectrum of ^{192}Po.

4 Intruder states and the Pairing Vibration Model

One of the first issues which must be clarified when trying to understand the difference between the very light Po isotopes and the heavier ones is the structure of the first excited 0^+ state. As can be seen from figure 1, the position of the 0_2^+ state shows a very pronounced mass dependence, which seems strongly correlated with the general drop in the energies of the yrast and yrare states below ^{200}Po. This mass dependence is also strongly reminiscent of the observed behavior of the intruder 0^+ states in the light Pb isotopes, which most probably have a proton two-particle two-hole (π(2p-2h)) structure [1, 41].

In this respect, it is useful to estimate the position of the lowest π(4p-2h) configuration in the Po isotopes and its behavior with varying neutron number. A very good guide for such an estimate are the predictions of the Pairing Vibration Model [39]. The model can describe multi-particle multi-hole states built from strongly correlated pairs of nucleons, as resulting from the pairing interaction.

A detailed discussion of the Pairing Vibration Model can be found e.g. in ref. [39]. We mention here that the building blocks of the model are pairs of correlated particles and holes, coupled to spin $J^\pi = 0^+, 2^+ ....$ We will concentrate only on the 0^+ states. The pair of correlated particles is called a pair addition phonon, with energy $\hbar\omega_+$, and a pair of correlated holes is called a pair removal phonon, with energy $\hbar\omega_-$. The multiphonon states are labeled by the number of phonons of both types, (n_-,n_+). The reference zero-phonon state is, in the present case, the ground-state of an even-mass Pb nucleus with N neutrons. The states containing phonons of only one type are, for (n_-,0) the ground-states of the Hg, Pt, Os,..., nuclei, and for (0,n_+) the ground-states of the Po, Rn, Ra,..., nuclei with the same neutron number N. The energies $\hbar\omega_+$ and $\hbar\omega_-$ are taken to be equal and determined from the binding energies (B.E.) of the Hg and Po nuclei relative to the Pb binding energy.

$$\begin{aligned} \hbar\omega_+ &= \text{B.E.}(A_0+2) - \text{B.E.}(A_0) - 2\cdot\lambda \\ \hbar\omega_- &= \text{B.E.}(A_0-2) - \text{B.E.}(A_0) + 2\cdot\lambda, \end{aligned} \tag{3}$$

where A_0 indicates the closed shell Pb nucleus and λ is determined from the condition that the two energies are equal. From the energies of the two-phonon states and their deviations from the harmonic predictions, one can extract the interaction between pairs of quanta, V_{++} from the (0,2), V_{--} from the (2,0) and V_{+-} from the (1,1) state. We exemplify in Fig. 6 the predictions of this model for the multiphonon states around ^{198}Pb (N=116). The binding energies are taken from ref. [44]. The anharmonicities are large, of the same magnitude as the phonon energy. Nonetheless, the binding energy of the Ra nucleus belonging to the chain (the (0,3) state) is correctly predicted using the $\hbar\omega$ and V_{++} values indicated in the figure. For the chains corresponding to a larger number of neutrons, where masses for the Th nuclei (Z=90) are known or estimated, they are also very well reproduced by the model. The binding energies of the Os and W nuclei with N=116 and actually for the whole range N=120–108, where data exist, are underestimated (in absolute value). Most probably, additional deformation effects are responsible for the extra binding energy of these nuclei.

The prediction of the model for 4p-2h states in the Po nuclei are summarized in Fig. 7, and are compared with the experimental energies of the first excited 0^+ states. It is seen that the agreement is remarkably good, and supports the assignment to the 0^+ states of a π(4p-2h) structure. Unfortunately, for the very light isotopes ^{194}Po and ^{192}Po, where the 0^+_2 state is not known experimentally and a model prediction would be very welcome, there are no experimental values for the ^{196,194}Rn masses needed to determine the parameters of the model. An extrapolated mass-value is available for ^{196}Rn and a corresponding prediction for the (1,2) state in ^{194}Po can be made, but the errors involved are too large.

Some additional remarks are required. The Pairing Vibration model involves basically a spherical picture (nuclei around closed shells with a large shell gap) and it describes, in principle, states which have a pure n(2p)0^+-m(2h)0^+ structure. Nevertheless, the excitation energies of the phonon states are calculated using the values of the experimental masses, which clearly include other effects than those due to pairing. For example, additional ground-state binding energy can be gained from deformation and from effects of the quadrupole interaction (as a leading term). These effects are clearly included in the phonon energies $\hbar\omega_{+,-}$ and in the anharmonic correction terms V_{++} and V_{--}. Furthermore, the third correction term, V_{+-}, is deduced directly from the position of the 2p-2h state in the closed shell nucleus, as compared to the harmonic prediction. In the case of the Pb nuclei, the intruder 2p-2h states have been interpreted as having an oblate deformation and their mass behavior as being mainly determined by the effects of the quadrupole interaction [2]. The predictions made for the multiphonon states include, therefore, effects due to deformation and quadrupole correlations. The states from which the parameters of the model are extracted are all either spherical or have a moderate oblate deformation. Consequently, it seems likely that multiphonon states with oblate deformation will be better described by the model in this particular region than states with prolate deformation.

The predictions of the Pairing Vibration Model can be applied not only to estimate the energies of multi-particle multi-hole states, but also to the analysis of the hindrance factors measured in $\alpha-$decay in this region [25, 45, 46]. A schematic decay process connecting the ground-state of a parent ^{A}Po nucleus with the ground-state and intruder state of the daughter $^{A-4}$Pb nucleus is shown in figure 8. The matrix elements for the $\alpha-$decay between different mp-nh configurations are denoted T_1,...,T_4 in the figure.

In the analysis it is supposed that in both nuclei the ground-state and the 2p-2h excitation built on it are mixed. We used the method outlined in refs. [46, 47] to estimate the mixing between the 4p-2h and the ground-state configuraton in the Po isotopes as a function of the experimental hindrance factors and the mixing between the 2p-2h and the ground-state in the corresponding Pb daughters. The difference as compared to refs. [46, 47] lies in the value we chose for the ratio A=T_4/T_1. In the Pairing Vibration Model this ratio should be $\sqrt{2}$ in absolute value, since it compares the transition from the two-phonon to the one-phonon state with the transition from a one-phonon to the zero-phonon state. The quantities needed to calculate the mixing of the two 0^+ configurations in a Po parent are: the experimental hindrance factors measured in $\alpha-$decay (HF), the (relative) values of the matrix elements T_1...T_4 which intervene in the calculation of the hindrance factors in the two-state picture and the mixing between the ground-state and intruder configurations in the daughter Pb nucleus. Making use of the g.s. (g) and intruder (i) configurations, the states involved in the $\alpha-$decay of a Po parent to a daughter Pb nucleus can be written as:

$$\begin{array}{lrcrlrcr} \mathbf{Po}: & \text{g.s.} & = & a\,|g\rangle + b\,|i\rangle & \mathbf{Pb}: & \text{g.s.} & = & c\,|g\rangle + d\,|i\rangle \\ & 0_2^+ & = & -b\,|g\rangle + a\,|i\rangle & & 0_2^+ & = & -d\,|g\rangle + c\,|i\rangle \end{array} \tag{4}$$

We introduce the notations: R=$\sqrt{\text{HF}}$, A=T_2/T_1, α =b/a (mixing in Po), β =d/c (mixing in Pb) and make the assumption that T_3 =0 and $|\text{T}_4/\text{T}_1|^2 = 2$, as given by the Pairing Vibration picture. The expression for the quantity which describes the mixing in Po, α, becomes (keeping only the solution with physical meaning):

$$\alpha = \frac{1+\beta R}{\sqrt{2}(R-\beta)} - A/\sqrt{2} \tag{5}$$

In the case when both in Po and in Pb the g.s. and 0_2^+ states are unmixed, the factor A can be deduced from the experimental hindrance factor as HF=A^{-2}. Supposing that this situation approximately holds for ^{198}Po and ^{194}Pb, we obtain A$\simeq$0.6.

The results for the mixing between the spherical and intruder configurations in the ground-state of the Po isotopes are tabulated in Table 2. From the mixing amplitudes and the energy $\text{E}(0_2^+)$, the mixing matrix element $\text{V}(0^+)$ and energy shift δE produced by mixing can be calculated. The input data are the experimental hindrance factors measured in $^{A}\text{Po}\rightarrow{}^{A-4}\text{Pb}$ $\alpha-$decay taken from Refs. [45, 48], the mixing between the 2p-2h and the ground-state in the Pb isotopes taken from Ref. [42], the experimental energies $\text{E}(0_2^+)$ in the Po isotopes taken from Ref. [25], together with the assumptions outlined above concerning the transition amplitudes T_1,...,T_4. The squared mixing ratios in Po and Pb, α^2 and β^2, are given in the form $\frac{b^2}{a^2}$ and $\frac{d^2}{c^2}$, respectively, with the notations of eq.(5). For the discussion of the mixing calculations concerning the states marked with an asterisk in Table 2, see section 6.1.

A remarkable result of the mixing calculations for the 0^+ states is that for ^{192}Po the spherical (2p-0h) and intruder (4p-2h) structures are inverted, that is, the structure of the ground state changes abruptly from mainly spherical in ^{194}Po to mainly intruder in ^{192}Po.

One further comment is due at this point. The above discussion was based on the assumption that there are only two 0^+ configurations involved in the $\alpha-$decay process. Their mixing in both the parent Po and in the daughter Pb nuclei is responsible for the observed hindrance factors. In a very recent work concerning the $\alpha-$decay of ^{192}Po [49], the population of a *third* low-lying 0^+ state in ^{188}Pb was reported. It is interpreted as being the band-head of the low-lying collective band already observed in-beam [7], which is supposed to have a prolate deformation and arise from a proton 4p-4h excitation. The population of a 4p-4h configuration in ^{188}Pb should be strongly favoured in the $\alpha-$decay proceeding from a dominant proton 4p-2h component in the ground-state of ^{192}Po. We will consider in this case all *three* low-lying 0^+ configurations in ^{188}Pb, which are expected to mix and influence the values of the hindrance factors. Noting by T_5 the amplitude for the decay 2p-0h$\rightarrow$4p-4h, and by T_6 the amplitude for the process 4p-2h$\rightarrow$4p-4h, we can assume $\text{T}_5 \simeq 0$ and the Pairing Vibration Model predicts a ratio $|\text{T}_6/\text{T}_2|^2 = 2$. Matrix elements for the interaction between the proton 0p-0h and the 2p-2h configurations in the light Pb isotopes were extracted in Ref. [42] for $^{194-190}$Pb, and found to be in the range 50$\div$80 keV with an apparently increasing trend with decreasing mass. We use for the following discussion of ^{188}Pb a matrix element of 80 keV, similar to the one found for ^{190}Pb [42]. The same matrix element is used for the interaction of the 2p-2h and the 4p-4h configurations, which is a natural assumption based

on the shell-model. The interaction between the 4p-4h and 0p-0h configurations is expected to be very reduced and is neglected (for a similar study, see for example Ref. [50]). In this three-state mixing picture, unperturbed energies of 550 keV for the 2p-2h configuration and 730 keV for the 4p-4h configuration plus the interaction matrix elements considered above, are consistent with the experimental energies of 571(4) keV for the oblate and 776(12) for the prolate state [49]. With the mixing amplitudes obtained from this three-state mixing in ^{188}Pb and the mixing of 80% 4p-2h and 20% 2p-0h for the ground-state of ^{192}Po, hindrance factors HF=0.9 for the oblate state and HF=0.3 for the prolate state are obtained. This result compares qualitatively well with the reported hindrance factors [49] of 0.67(10) for the 2p-2h (oblate) and 0.22(8) for the 4p-4h (prolate) state. Alternatively, if we use these experimental hindrance factors to determine the mixing between the 2p and 4p-2h configurations in the ground-state of ^{192}Po, a structure of 84% intruder and 16% spherical components is obtained. This is only a minor change to the result listed in Table 2. Our values are also consistent with the result of Ref. [49], in which a 63% intruder-state component was found in the ground-state of ^{192}Po, although some of the assumptions used were different.

In summary, the good agreement between the predictions of the Pairing Vibration Model and the experimental energies of the 0_2^+ states strongly suggest that these states are of 4p-2h structure. A simple two-state mixing calculation, which makes use of information obtained mainly in $\alpha-$decay experiments, leads to the conclusion that the dominant ground-state configuration changes from 2p-0h to 4p-2h between ^{194}Po and ^{192}Po. This conclusion is consistent with the new results obtained for the $\alpha-$decay of ^{192}Po [49]. We will make further use of the results obtained with this method in Section 6.1. Further arguments for this interpretation, as well as information concerning the deformation of the intruder structure are obtained from Potential Energy Surface calculations.

5 Potential Energy Surface calculations

Early Nilsson-Strutinski calculations by May, Pashkevich and Frauendorf [51] already predicted the appearance of deformed shapes at low energies in the very light Po isotopes (A$\leq$192). Nonetheless, they suggested that the heavier isotopes with A=194, 196,..., should be interpreted as anharmonic vibrators. For ^{192}Po, a minimum at oblate deformation ($\epsilon = -0.2$) was found, and in the lighter isotopes ^{190}Po and ^{188}Po a well deformed prolate minimum ($\epsilon = 0.25$) was predicted as well. It was noted in Ref. [51] that the choice of pairing parameters and of the parameters of the Woods-Saxon potential influences quite strongly the predicted relative energies of the minima corresponding to different shapes. Nevertheless, the systematics of the changes in the nuclear shape were found to be much less sensitive to the input parameters.

A recent study of the mercury and lead isotopes by Nazarewicz [15] proved that deformed mean field calculations, in a refined version, are able to give good quantitative predictions of the energies of the deformed 0^+ states in the chains of isotopes studied.

We have performed two different sets of calculations for the Po isotopes, restricting either to axial symmetric shapes, or taking into account non-axial symmetric shapes (triaxial) as well. The calculations are based on the Strutinski shell correction method [52], using a deformed average Woods-Saxon potential [53] and follow along the line described in Ref.[54]

(axial symmetric shapes) and [55] (triaxial shapes). The macroscopic energy was calculated with the Myers-Swiatecki [56] liquid drop model formula. In the treatment of the pairing, the Lipkin-Nogami method [57] was used for an approximate number projection. For each β_2-value, the total energy was minimized with respect to β_4 [54, 55, 58]. We have used two different sets of parameters of the Woods-Saxon potential, in order to investigate the dependence of the results on potential parameters. For the parameter sets used, we found some dependence in the relative energies of the different minima, but the same overall picture concerning coexisting configurations.

The potential energy surfaces obtained for several Po isotopes, when non-axial symmetric shapes are studied, are shown in Figures 9 and 10. The minima are marked with dots. The surfaces are reflection-symmetric with respect to the axes at $\gamma = 0°$ and $\gamma = -60°$. In Figure 9, the surfaces obtained from the calculation which takes into account only axial symmetric shapes are shown as well. Interestingly, the oblate-prolate shape coexistence, obtained for the potential-energy surfaces at axial shapes and small quadrupole deformation, does not represent true coexistence, but reflects only the $\gamma-$softness of the surface. This can be understood from simple topology, that requires a minimum at non-zero quadrupole deformation in order to build up a barrier between prolate and oblate shapes. Hence, the lowest minimum found for the heavier isotopes at β_2=0.05–0.09 (see Figure 9) has no well-defined $\gamma-$coordinate. This feature is nicely seen in ^{202}Po (as well as for heavier Po-isotopes not shown here), where the energy of the lowest minimum is essentially indifferent to the whole range of $\gamma-$values ($\gamma = -60° - 0°$). With decreasing neutron number, the minimum becomes more localized on the prolate side ($\gamma = 0°$), but remains very soft with respect to the $\gamma-$values at given β_2. The heavier Po isotopes are, therefore, predicted to be $\gamma-$soft in the ground state. The quadrupole deformation of this minimum is slightly increasing towards mid-shell but stays always below $\beta_2 = 0.1$ and is found in all the isotopes studied here. One expects states of mainly vibrational character to be associated with this minimum.

A deformed minimum with $\beta_2 = -0.20$ is found at oblate shapes in the mass range A=202–186. It is apparent as a 'shoulder' already in the PES for ^{202}Po and becomes more pronounced in the lighter isotopes. In ^{192}Po it appears clearly separated from the rest of the $\beta - \gamma$ plane and constitutes the absolute minimum. We note that the barrier separating the oblate and nearly spherical minima via triaxial shapes tends to decrease with decreasing neutron number. Since the energy difference between the two configurations is also predicted to decrease, their mixing can be expected to increase substantially with decreasing mass.

A third minimum with large prolate deformation $\beta_2 \sim 0.3$ appears in ^{190}Po and becomes the absolute minimum in ^{186}Po. In ^{184}Po, the oblate minimum disappears and the energy difference between the prolate minimum and the nearly spherical one decreases. Below N=100 (not shown in Fig. 10), there is a rapid change in the minima, and for neutron number N=98 a large shell correction at prolate shape results in the presence of a prolate minimum only.

With a further decrease of the neutron number, the structure close to the spherical shape becomes lowest again and the prolate minimum disappears around N=94. The very light Po isotopes (N$\leq$94) are predicted to be nearly spherical in their ground states, similar to the result obtained in Ref. [15] for the Hg isotopes.

Information about the structure of the different minima can be obtained from inspection of the Nilsson diagrams at the corresponding deformations. The shape-driving properties of different configurations are more clearly obtained from the study of the shell-correction

energy for neutrons and protons separately. We show in Figs. 11 and 12 the shell- and pairing-correction energy obtained for neutrons in the range N=126–104 and protons, respectively. We include in Fig. 12 calculations for proton numbers Z=76–86, but we will concentrate in our discussion on the Po isotopes.

For Z=84, the separate proton surface reveals a deep but also $\gamma-$soft surface at spherical shape and a 'shoulder' present in the PES around $\beta_2 = -0.2$. The 'shoulder' at oblate shape corresponds to the 4p-2h excitation with respect to the spherical Pb-core. Prolate shapes are not favoured at all, as is evident from the maximum of the shell correction at deformed prolate shapes. Once the neutrons start to favour deformed shapes at oblate deformation ($N \approx 114$), the combined shell-correction of protons and neutrons results in the onset of oblate minima in the total PES. The evolution of the oblate minimum with neutron number seems to be due to the increasing localization of the neutron shoulder at oblate deformations $\beta_2 \sim -0.2$. A certain softness in the direction of oblate shapes remains with decreasing neutron number, but the oblate minimum in the total PES disappears at N=102, simultaneously with the shoulder in the neutron PES.

In a similar way it was found that the $\gamma-$soft region at small deformations is a result of the rather large proton shell correction at spherical shapes combined with $\gamma-$softness. Once the neutrons favour prolate shapes, the small deformation minimum moves from oblate to prolate shape but remains $\gamma-$soft. The position of this minimum is a nice indicator of the change in the oblate-prolate energy balance of the neutrons.

The origin of the prolate minimum for N=106–100 can be associated with the very pronounced shell correction for midshell neutrons, where the quadrupole–quadrupole interaction has its maximium. The midshell quadrupole collectivity is very coherent (large shell-correction) and will always result in a minimum, even in the absence of a favoured proton shell-correction energy. Favoured gaps in the Nilsson diagram that are associated with additional energy gain at prolate shape appear for the neutron numbers N=98, 102 and 106. Although the neutrons above mid-shell favour oblate shapes, there is much less coherence in the quadrupole collectivity compared to prolate shapes. Evidently, there is no symmetry between prolate and oblate shapes, reflecting sizeable differences in the shell structure. Since in the final PES calculations, protons and neutrons are forced to have identical shapes, the quadrupole collectivity of protons and neutrons at a given deformation has to add up. Therefore, the above separation of proton and neutron effects is in close analogy to the scheme discussed in Ref. [59].

A brief inspection of Figs. 11 and 12, combined with the existing information on shape coexistence in the Pb region [1, 3, 4, 5, 6, 7, 8, 9, 10, 11, 12, 13, 14], stresses the conclusion that secondary minima in the PES (shape coexistence) are related to the distinct balance of prolate and oblate energy difference of *both* protons and neutrons for a given configuration. Based on this observation, it is interesting to note that the Rn isotopes should be expected to exhibit the same variety of coexisting shapes as the Po and Pb isotopes (close to spherical, oblate and prolate). From our study, the oblate configuration should be quite low already in ^{198}Rn, but the experimental information is not conclusive yet [13, 14].

The excitation energies found in our study of the various low-energy, shape-coexisting 0^+ configurations in the Po isotopes, are summarized in Figure 13. Only the isotopes heavier than A=184 (N=100) are shown. The energies of the oblate minima found in the PES correspond rather well to the experimental energies of the 0_2^+ states. We mention that no effect of the

zero-point vibrations was taken into account when calculating the relative energies of the different minima.

Since the agreement of the energies predicted by the PES calculations with the experimental energies is found to be good (see Fig. 13), we will use these predictions as a guide for the position of the 0^+ states in ^{194}Po and ^{192}Po, where no experimental values are available. It can be concluded from our study that the ground-state of ^{192}Po is most probably oblate deformed, but mixing with the nearly spherical configuration is to be expected.

The results of the PES calculations definitely support the manifestation of shape coexistence in the Po isotopes. The perturbation in the systematics of the light isotopes can be then interpreted as resulting from the lowering of the deformed 0^+ configuration and its associated band and their gradual mixing with the nearly spherical configurations. This effect is described more quantitatively in the next section.

6 Mixing Calculations

6.1 Two-state mixing

From the discussion of the previous subsections and anticipating the results of Sect. 6.2, it is seen that neither PCM (with only one core) nor IBM-2 calculations can describe the full range of phenomena met in the Po isotopes with neutron number varying between N=126 and N=108.

Nevertheless, as already pointed out in section 4 for the 0^+ states, important information about the intruder structure and its mixing with the regular states can be extracted from the experimental data, making use of a simple two-state mixing picture. We use several assumptions.

- the PES calculations give a good description of the evolution of deformation and the relative energies of the structures with different deformations in this mass region,
- there are two structures which determine the evolution of the systematics of the Po isotopes below mass number A=200. The first structure corresponds to the one met in the heavier isotopes, is nearly spherical and is mainly due to the two-proton degrees of freedom coupled to the neutron collective excitations. The second structure comes into play around mass number A=200 and is strongly lowered in energy with decreasing neutron number. It is an intruder band built on the first excited 0^+ state observed in $\alpha-$decay and β^+/EC studies. It is most probably a deformed structure of constant deformation,
- the hindrance factors measured in $\alpha-$decay experiments [45, 48] give information about the mixing of the nearly spherical and intruder 0^+ states. For a two-state mixing calculation we use the mixing amplitudes extracted from the hindrance factors and (i) the experimental energies of the two 0^+ states, or (ii) the predicted unperturbed energies in the cases where the second 0^+ state was not observed. The unperturbed energies of the two 0^+ states (in case (i)), as well as the shift δE=E$_u$-E$_p$ and the mixing matrix element (in both cases) can be deduced,

- the yrast sequence of excited states ($2^+ - 8^+$) experimentally observed in ^{192}Po corresponds to the deformed intruder band. Besides the 0^+ ground state, which is significantly mixed with the spherical structure, the intruder band seen in ^{192}Po is assumed to be pure,

- The structure of the intruder band, deduced from the yrast sequence in ^{192}Po corrected for mixing of the 0^+ bandhead with the spherical 0^+ state (not observed), is assumed to be unchanged over the limited mass range A=198–192.

We give below some useful relations used for the two-state mixing calculations, with evident notations (a and b are the amplitudes of the two initial configurations in the wave functions of the final states, and $b \leq a$).

$$\begin{array}{lll} \delta E = \frac{b}{a} V & \delta E = b^2 \Delta E_p & \delta E = \frac{b^2}{a^2 - b^2} \Delta E_u \\ \Delta E_p = \frac{1}{ab} V & \Delta E_p = \frac{1}{a^2 - b^2} \Delta E_u & V^2 = \delta E (\delta E + \Delta E_u) \quad , \end{array} \tag{6}$$

where δE is the (positive) difference of the energies of the unperturbed and mixed states, ΔE_u is the energy spacing between the unperturbed states, ΔE_p is the energy spacing between the mixed states ($\Delta E_p = \Delta E_u + 2\,\delta E$) and V is the mixing matrix element.

The energy depression of the ground state of ^{192}Po was found to be $\delta E = 59$ keV, using the mixing amplitudes given in Table 2 and the unperturbed energy spacing $\Delta E_u = 185$ keV of the two 0^+ configurations, predicted by the PES calculations. The energies in the $0^+ - 2^+ - 4^+ - 6^+ - 8^+$ sequence of the intruder band are, therefore, deduced to be 203-546-984-1502 keV, respectively. With the same type of input data for ^{194}Po and using the value $\Delta E_u = 142$ keV, the ground-state energy shift δE was deduced to be 44 keV in this nucleus. The experimental energies of the excited levels were corrected for this shift. On the unperturbed 0_2^+ state, the intruder band is built with the structure obtained from ^{192}Po. Comparing the predicted position of the intruder state with a given J^π with the energy of the experimental state with the same spin and parity closest to it, the energy shift due to the mixing of the two J^π configurations was calculated. The unperturbed position of the spherical state with the same spin-parity and the mixing matrix element were deduced.

Using the above procedure, we performed mixing calculations between the intruder and nearly spherical band with spins $0^+ - 8^+$ for the other two isotopes, ^{198}Po and ^{196}Po, which, together with ^{194}Po cover the transition between the 'regular regime' of the heavier isotopes and the more collective one found in ^{192}Po.

The results of the calculations are summarized in Table 3. The unperturbed energies of the spherical and intruder states with spin $0^+ - 8^+$ and the mixing matrix elements are listed.

The unperturbed energies of the spherical and intruder structures, deduced from the above calculations, are also shown in Figure 14. The results of the mixing calculation look quite reasonable: the behavior of the unperturbed energies is smooth and the mixing matrix elements seem to follow a specific pattern, which is not understood as yet. Besides, the reconstructed systematics of the spherical (regular) states show good agreement with the predictions of the Particle-Core model. No notable increase in collectivity is noticed from the behavior of the unperturbed spherical $2^+, 4^+, ...$ states.

The consistency of the results is quite remarkable given that the different approximations involved are not expected to hold rigorously (e.g. that the HF's for transitions within an $\alpha-$decay chain do not depend notably on the deformations of the states involved, or that the relative transition probabilities T_1,...,T_4 used in section 4 follow the Pairing Vibration predictions and do not change with the mass number, or that the structure of the intruder band is not changing between ^{192}Po and ^{198}Po).

It is interesting to stress that the deduced mixing matrix elements show a characteristic spin-dependence, as seen in Fig. 15. This behavior is consistent with the pattern which can be inferred for ^{190}Pb from Refs. [42] and [9]. Indeed, the matrix elements extracted in Ref. [42] for the interaction between intruder and spherical states with $J^\pi = 0^+, 2^+$ show an increase with spin-value from $V(0^+) \simeq 80$ keV to $V(2^+) \simeq 200$ keV. Matrix elements for the mixing of the similar states with $J^\pi = 4^+, 6^+$ are not known, but for the interaction of the 8^+ states a value of the order of $V(8^+) \simeq$10 keV was estimated in Ref. [9] (the matrix element was extracted either for mixing between the 2p-2h and 0p-0h 8^+ states or for the mixing between the 2p-2h and 4p-4h states; since in a shell-model picture the two matrix elements should be equal, the ambiguity in the structure assignment for the 8^+ states involved does not change our conclusion).

The understanding of this spin-dependent 'interaction pattern' certainly deserves further study.

6.2 An IBM-2 treatment

The mixing of a regular band and a deformed band has been well reproduced within the proton-neutron Interacting Boson Model (IBM-2) for several isotopic chains, e.g., the Hg and the Mo isotopes [60, 61, 62]. The general formalism, described in Ref. [60], involves two separate calculations, one for $N_\pi = \frac{|Z-Z_0|}{2}$ (where Z_0 is the shell closure for the protons) and one for $N_\pi = \frac{|Z-Z_0|}{2} + 2$ (two protons excited across the major shell gap), plus a mixing calculation. In the former two independent calculations, the standard IBM-2 Hamiltonian (i.e, Eq. 7) is diagonalized in the appropriate space for each case. In the mixing calculation we form the matrix elements of the mixing Hamiltonian (Eq. 10) with the wave functions of the two separate configurations and diagonalize the resulting matrix. Besides the strength parameters of the mixing Hamiltonian, the mixing calculation requires another parameter, called Δ, which gives the energy needed to excite a proton boson, i.e., a two-proton configuration, into the next major shell.

The standard IBM-2 Hamiltonian is of the form:

$$\hat{H} = \epsilon_\pi \hat{n}_{d_\pi} + \epsilon_\nu \hat{n}_{d_\nu} + \kappa \hat{Q}_\pi \cdot \hat{Q}_\nu + \hat{V}_{\pi\pi} + \hat{V}_{\nu\nu}, \tag{7}$$

where ϵ_π and ϵ_ν are the d boson single-particle energies, which we take to be equal, and $\hat{Q}$ is the boson quadrupole operator which we take to be of the form:

$$\hat{Q}_\rho = \left(d^\dagger \times s + s^\dagger \times d\right)^{(2)}_\rho + \chi_\rho \left(d^\dagger \times \tilde{d}\right)^{(2)}_\rho \ , \ \rho = \pi, \nu \tag{8}$$

The like-particle interaction is:

$$\hat{V}_{\rho\rho} = \sum_{L=0,2,4} \frac{1}{2}(2L+1)^{\frac{1}{2}} C^\rho_L \left[(d^\dagger \times d^\dagger)^{(L)}_\rho \cdot (\tilde{d} \times \tilde{d})^{(L)}_\rho\right]^{(0)} \ , \ \rho = \pi, \nu. \tag{9}$$

The mixing Hamiltonian is taken to be of the form:

$$\hat{H}_{mix} = \alpha \left(s_\pi^\dagger \times s_\pi^\dagger + s_\pi \times s_\pi \right)^{(0)} + \beta \left(d_\pi^\dagger \times d_\pi^\dagger + \tilde{d}_\pi \times \tilde{d}_\pi \right)^{(0)} \quad . \tag{10}$$

In the light of the previous discussion concerning the shape coexistence phenomenon in the Po nuclei, we attempt an IBM-2 description of the isotopes with mass number A=200–192 in terms of a 'regular' configuration (one proton boson and $N_\nu = \frac{126-N}{2}$ neutron-hole bosons) and a deformed intruder configuration (three proton bosons and $N_\nu = \frac{126-N}{2}$ neutron-hole bosons), which gradually mix. Figure 16 shows the results of the best IBM-2 fit obtained for the Po isotopes, compared with the experimental data. For each state, the amount of regular (thin line) and intruder (thick line) components is shown. In order to further check the two-state mixing picture of the previous subsection, we have plotted only the amount of the first regular and intruder configuration for a given J^π, respectively. We note that the IBM fit to the 'regular' band is not realistic for some of the 8_1^+ states, which are of two-proton structure and, hence, are outside of the model. On the other hand, the mixed results obtained for the configurations of lower angular momentum are in quite reasonable agreement with experiment.

The mixing matrix elements used in the IBM-2 calculation are presented in Fig. 17. The spin dependence is quite different from the one found in the two-state mixing approach of Sect. 6.1 and Fig. 15.

The fit was obtained under the condition that all parameters for all nuclei fitted are held constant, except for the parameter Δ. In order to obtain a good description of the experimental data, Δ had to be varied from 1.5 MeV for ^{200}Po to 0.55 MeV for ^{192}Po. The parameters are given in Table 4. Thus, in this analysis, the lowering of the deformed band arises mainly from the decrease in the energy required to excite the two protons across the Z=82 shell gap, which is related to the parameter Δ. This result is just the opposite to that found for the Hg isotopes [61], where Δ had to be held constant at 4.0 MeV and the deformed band fell in energy due to the increased collectivity, i.e. increasing $N_\pi N_\nu$ (larger value of N_π for the intruder band times an increasing value of N_ν). If the former interpretation is correct for the Po isotopes, then it would suggest that the collective structures of the Hg isotopes and the Po isotopes are quite different.

The study of the coexistence of regular and intruder configurations and their mixing can be embedded in a larger framework using particle-hole symmetry concepts and intruder spin [17, 18, 19]. The intruder 4p-2h structure in Po and the regular 6h excitations in the Os isotopes with the same neutron number belong both to the I=3/2 multiplet ($I_z = 1/2$ and $-3/2$, respectively) and are thus expected to be very similar. It is important to stress that, as I-spin symmetry implies that I is a good quantum number, mixing between regular and intruder configurations (with different I) within a given nucleus will destroy to some extent the similarity of the bands which are supposed to belong to an I-spin multiplet. The usefulness of the concept lies in the idea that one can extrapolate the properties of a well-studied and ideally unmixed *ground-state band* of a particular nucleus with ($I,I_z=\pm I$), to *excited bands* in other neighboring nuclei but belonging to the same multiplet (members with $|I_z| < I$) and use it as a starting point for a study of the mixing between regular and intruder configurations in those nuclei. In the particular case of the Po intruder states, the experimental information is scarce and most of the band members observed are expected to be mixed with the spherical

configurations. Along the lines of the above discussion, we make use of the rather large data set consisting of energies and E2 transition probabilities for the ground- and $\gamma-$bands of the Os isotopes in order to determine a reliable set of parameters which are well-suited for the description of the unmixed Po intruder bands.

We have thus performed another set of mixing calculations, in the framework of the IBM-1. As a first step, we simplified the calculations by approximating the regular and intruder structures with the best suited IBM-1 dynamical symmetry limits (U(5) and SU(3), respectively) and imposed the condition that all the parameters, including Δ, be held constant over the neutron range N=108–114. As this rather simplistic calculation already gives promising results, we proceeded with a more realistic IBM-1 study where for each individual Po intruder band we used the parameters best suited to describe the 6h structures of the Os I=3/2 partner isotope.

We realize that IBM fits are, in general, not unique, but we tend to favor a parameter choice in which Δ is kept constant - if possible at all - as being closer to the correct underlying physics. That is, it seems physically plausible that the excitation gap Δ, which can be related to the shell gap at Z=82, will not vary much with varying neutron number N_ν. Work on this point is in progress and will be presented in a forthcoming paper [63].

7 Conclusions

In the present paper, we have carried out a detailed investigation of the nuclear properties of the Po nuclei in the mass range $192 \leq A \leq 210$. To this aim, we have studied various complementary theoretical approaches in order to be able to reach a number of conclusions in as reliable a way as possible.

A careful Particle-Core Coupling Model (PCM) study has provided a good description of the Po isotopes above mass number A=200, where only the 'regular' proton and neutron excitations play a role. The Bi isotopes with the corresponding neutron numbers have been treated simultaneously with the Po isotopes, in order to determine a number of model parameters from the data which are most relevant to them and to strive as much as possible for consistency when applying the PCM. For the Po isotopes below A=200, as well as the corresponding Bi isotopes, the experimental data are too scarce to provide a reliable determination of the model parameters, and some extrapolation was needed. It was nevertheless shown that the Particle-Core Model cannot describe the transition down to ^{192}Po if one uses the same configuration space as for the heavier isotopes.

The assignment of a 4p-2h structure of the second excited 0^+ states in the light Po isotopes has been supported by predictions of the phenomenological Pairing Vibration Model. The predicted energies agree well with the experimental ones and both show an energy behavior with mass number consistent with the shell-model predictions for intruder configurations. Using the Pairing Vibration Model and the experimental hindrance factors (HF) measured in the $\alpha-$decay of the parent Po to the daughter Pb nuclei, the mixing amplitudes between the 4p-2h and regular 2p configurations have been deduced. The ground state of ^{192}Po is found to be of mainly intruder character.

This interpretation was further supported by the results of Potential Energy Surface (PES) calculations for the Po isotopes. A pronounced minimum in the PES has been obtained in

the deformed mean field picture, corresponding to 0^+ states with an oblate deformation and a likely 4p-2h structure. The oblate 0^+ states are strongly lowered in energy with decreasing neutron number, as compared with the nearly spherical ground state minimum. The calculated energies correspond well to the experimental energies of the 0_2^+ states. In ^{192}Po, the oblate minimum has been predicted to become the lowest one, to remain so until ^{188}Po and to disappear for the isotopes lighter than ^{186}Po. Furthermore, a strongly deformed prolate minimum was predicted to appear in ^{190}Po and to become the ground state configuration in ^{186}Po. According to the predictions of the PES calculations, in ^{190}Po, ^{188}Po and ^{186}Po the 0^+ oblate, prolate and nearly spherical configurations are all expected to appear below 800 keV, 300 keV and 800 keV excitation energy, respectively.

It can be, therefore, put forward that in the light Po nuclei the interplay of the spherical structures and an intruder band, which is strongly lowered in energy with decreasing neutron number, is responsible for the observed perturbation of the systematics. In order to describe this evolution, two approaches were used.

(i) A simple two-state mixing approach, involving the intruder and spherical configurations, was used in order to describe the evolution of the systematics between ^{200}Po and ^{192}Po. The structure of the 'reference' intruder band is inferred from the experimental level scheme of ^{192}Po, correcting for the mixing between the 0^+ intruder and spherical configurations. The unperturbed energies of the spherical and intruder states and the mixing matrix elements can thus be deduced. The behavior of the spherical states with mass number agrees well with the one expected in a Particle-Core Model picture, and leads to the conclusion that the two-particle and collective aspects still keep their identity in the light Po isotopes. A picture in which the two-proton degrees of freedom and the neutron ones 'melt' in a common collective behavior, as proposed in previous PCM studies, does not seem to be valid.

(ii) The IBM calculations take into account two different structures and their mixing, and are able to reproduce rather well the evolution of the energies of several states for mass numbers below A=200, but the structure of the 'regular band' is rather poorly described for the nuclei above this mass number.

As shown by the model calculations on the light Po nuclei presented in this paper, further efforts are still needed in order to obtain an even more consistent description of the heavier (A=200–210) as well as of the lighter (A=192–200) isotopes. A unified treatment of the spherical and intruder structures in the framework of the Particle-Core Model will be attempted in the near future. This can be done by the use of two subspaces, $^{\text{A-2}}$Pb+2p for the 'regular' structure and $^{\text{A+2}}$Rn$-$2h for the 4p-2h intruder configuration, and taking the mixing between the two subspaces explicitly into account. The clear differences between the Po and Hg isotopes, which can be described, in principle, as two particles or two holes, respectively, coupled to the same Pb core, will be investigated further in the Particle-Core Model.

The final conclusion of our detailed study of the light Po isotopes is that the strong perturbation evident in the systematics below A=200 is due to the mixing between two shape coexistent configurations. The intruder band gradually replaces the spherical states in the yrast sequence and becomes the ground state band in ^{192}Po. Direct experimental proof for the mixing, as can be obtained from measurements of transition probabilities involving the yrast and yrare states, would be a key check of our interpretation.

ACKNOWLEDGEMENTS

We gratefuly acknowledge fruitful discussions with N. Bijnens, J. Cizewski, G. Dracoulis, H. Grawe, M. Huyse, R. Julin, R. Liotta, W. Nazarewicz, R. Page, P. Van Duppen, W.B. Walters and J. Wood. This work has been supported by the IIKW and FWO-Flanders and by the NATO Research Grant CRG 96-0981. One of the authors (K.H.) is grateful to the EP-ISOLDE division and to CERN for financial support in the final stage of this work. One of us (B.R.B.) would like to thank the "Vakgroep Subatomaire en Stralingsfysica" of the University of Gent for its hospitality and the University of Gent for financial support during his stay in Belgium. B.R.B. and P.N. wish to acknowledge partial support by NSF grant No. PHY96-05192.

References

[1] J.L. Wood, K. Heyde, M. Huyse and P. Van Duppen, Phys. Rep. 215, 101(1992).

[2] K. Heyde, J. Jolie, J. Moreau, J. Ryckebusch and M. Waroquier, Nucl. Phys. **A466**, 189(1987).

[3] G.D. Dracoulis, B. Fabricius, A.E. Stuchbery, A.O. Macchiavelli, W. Korten, F. Azaiez, E. Rubel, M.A. Deleplanque, R.M. Diamond and F.S. Stephens, Phys. Rev. **C44**, R1246 (1991).

[4] S. King et al, submitted to Phys. Lett. B.

[5] M.P. Carpenter et al., Phys. Rev. Lett.**78**, 3650 (1997).

[6] M. Muikku et al., submitted to Phys. Rev. C.

[7] J.Heese, K.H.Maier, H.Grawe, J.Grebosz, H.Kluge, W.Meczynski, M.Schramm, R.Schubart, K.Spohr and J.Styczen, Phys. Lett. **302B**, 390 (1993).

[8] A. M. Baxter et al., Phys. Rev. **C48**, R2140(1993).

[9] G.D.Dracoulis, A.P.Byrne and A.M.Baxter, Phys.Lett. **432B**, 37 (1998).

[10] J.F.C. Cocks et al., accepted for publication in Europhysics Letters.

[11] K. Helariutta et al., Phys. Rev. **C54**, R2799(1996).

[12] N. Fotiades et al., Phys. Rev. **C55**, 1724(1997).

[13] R. Julin, priv. comm., 1997.

[14] R.B.E. Taylor et al., Phys.Rev. **C54**, 2926 (1996).

[15] W. Nazarewicz, Phys. Lett. B **305**, 195(1993).

[16] K. Heyde, C. De Coster, J. Jolie and J.L. Wood, Phys. Rev. **C46**, 541(1992).

[17] C.De Coster, K.Heyde, B.Decroix, P.Van Isacker, J.Jolie, H.Lehmann and J.L.Wood, Nucl.Phys. **A600**, 251 (1996).

[18] C.De Coster, B.Decroix, K.Heyde, J.L.Wood, J.Jolie and H.Lehmann, Nucl.Phys. **A621**, 802 (1997).

[19] H. Lehmann, J. Jolie, C. De Coster, B. Decroix, K. Heyde, J.L. Wood, Nucl. Phys. **A621**, 767(1997).

[20] K.Heyde, P.Van Isacker and J.L.Wood, Phys.Rev. **C49**, 559 (1994).

[21] L.A. Bernstein et al., Phys.Rev. **C52**, 621 (1995).

[22] W. Younes et al., Phys.Rev. **C52**, R1723 (1995).

[23] J.A.Cizewski and W.Younes , Z.Phys. A **358**, 133 (1997).

[24] W.Younes and J.A.Cizewski, Phys.Rev. **C55**, 1218 (1997).

[25] N. Bijnens et al., Phys. Rev. Lett. **75**, 4571(1995).

[26] National Nuclear Data Center, Brookhaven National Laboratory.

[27] A. Maj H.Grawe, H.Kluge, A.Kuhnert, K.H.Maier, J.Recht, N.Roy, H.Hubel and M.Guttormsen, Nucl. Phys. **A509**, 413(1990).

[28] N. Bijnens et al., Phys.Rev.C58, 754 (1998).

[29] D. Alber et al., Z. Phys. **A 339**, 225(1991).

[30] A.B. Quint et al., GSI-88-1, p.16 (1988); J.C. Batchelder et al., Phys. Rev. **C54**, 949 (1996); A. N. Andreyev et al., Z. Phys. **A358**, 63 (1997); J.C. Batchelder et al., Phys .Rev. **C55**, R2142 (1997).

[31] K. Heyde and P.J. Brussaard, Nucl. Phys. **A104**, 81(1967).

[32] K. Heyde and P. J. Brussaard, Nucl. Phys. **A112**, 494(1968).

[33] P. Van Isacker, K. Heyde, M. Waroquier and H. Vincx, Phys. Rev. **C19**, 498 (1979).

[34] J. Copnell, S. Robinson, J. Jolie and K. Heyde, Phys. Lett. **222B**, 1 (1989).

[35] J. Copnell, S. J. Robinson, J. Jolie and K. Heyde, Phys. Rev. **C46**, 1301 (1992).

[36] L. Trache, K. Heyde and P. von Brentano, Nucl. Phys. **A554** (1993) 118.

[37] A.M. Oros, Ph.D. Thesis, Köln 1996, unpublished.

[38] A. M. Oros, P.von Brentano, R.V. Jolos, L. Trache, G. Graw, G. Cata-Danil, B.D. Valnion, A. Gollwitzer and K. Heyde, Nucl. Phys. **A613** , 209 (1997).

[39] A. Bohr and B. Mottelson, *Nuclear Structure*, volume 2, W. A. Benjamin Inc. London, Amsterdam, 1975.

[40] C. Pomar, J. Blomquist, R.J. Liotta and A. Insolia, Nucl. Phys. **A515**, 381 (1990).

[41] P.Van Duppen, E. Coenen, K. Deneffe, M. Huyse, K. Heyde and P. Van Isacker, Phys. Rev. Lett. **52**, 1974 (1984).

[42] P.Van Duppen, M. Huyse and J.L. Wood, J. Phys. G **16**, 441 (1990).

[43] G.Neyens, S.Ternier, N.Coulier, K.Vyvey, R.Coussement and D.L.Balabanski, Nucl.Phys. **A625**, 668 (1997).

[44] G. Audi, O. Bersillon, J. Blachot and A.H. Wapstra, Nucl. Phys. **A624**, 1(1997).

[45] J.Wauters, N.Bijnens, P.Dendooven, M.Huyse, H.Y.Hwang, G.Reusen, J.von Schwarzenberg, P.Van Duppen, R.Kirchner, E.Roeckl, and the ISOLDE Collaboration , Phys.Rev.Lett.**72**, 1329 (1994).

[46] J.Wauters, N.Bijnens, H.Folger, M.Huyse, H.Y.Hwang, R.Kirchner, J.von Schwarzenberg and P.Van Duppen, Phys.Rev. **C50**, 2768 (1994).

[47] N.Bijnens, J.G.Correia, M.Huyse, H.Y.Hwang, R.Kirchner, G.Reusen, E.Roeckl, P.Van Duppen, J.von Schwarzenberg, J.Wauters, and the ISOLDE Collaboration, Phys.Scr. T56, 110 (1995).

[48] N. Bijnens, Ph.D. thesis, Leuven 1998, unpublished.

[49] R.G. Allatt et al., accepted for publication in Phys. Lett. **B**.

[50] K. Heyde and R.A. Meyer, Phys. Rev. **C41**, 280 (1990).

[51] F.R. May, V.V. Pashkevich and S. Frauendorf, Phys. Lett. **68B**, 113(1977).

[52] V.M. Strutinski, Nucl. Phys **A95**, 420(1967).

[53] S. Ćwiok, J. Dudek, W. Nazarewicz, J. Skalski and T. Werner, Comp. Phys. Comm. **46**, 379 (1987).

[54] W. Satula, S. Cwiok, W. Nazarewicz, R. Wyss and A. Johnson, Nucl. Phys. **A529**, 289(1991).

[55] W.Satula and R.Wyss, Phys.Scr. T56, 159 (1995).

[56] W.D. Myers and W. Swiatecki, Ark. Fys. **36**, 343(1967).

[57] H.C.Pradhan, Y.Nogami and J.Law, Nucl. Phys. bf A201, 357 (1973).

[58] W. Nazarewicz, M.A. Riley and J.D. Garrett, Nucl. Phys. **A512**, 61(1990).

[59] K. Heyde, C. DeCoster, J. Ryckebush and M. Waroquier, Phys. Lett. **B218**, 287 (1989).

[60] P.D. Duval and B.R. Barrett, Nucl. Phys. **A376**, 213(1982).

[61] A. F. Barfield, B.R. Barrett, K.A. Sage and P.D. Duval, Z. Phys. **A311**, 205(1983).

[62] M. Sambataro and G. Molnar, Nucl. Phys. **A376**, 201(1982).

[63] C. De Coster, B. Decroix, K. Heyde, H. Lehmann, J. Jolie, J.L. Wood, in preparation.

^{A}Po	$\hbar\omega_2$ [MeV]	ξ_2	$\hbar\omega_3$ [MeV]	ξ_3	G_{SDI} [MeV]	$\epsilon(1h_{9/2})$ [MeV]	$\epsilon(2f_{7/2})$ [MeV]	$\epsilon(1i_{13/2})$ [MeV]	$\epsilon(2f_{5/2})$ [MeV]	$\epsilon(3p_{3/2})$ [MeV]	$\epsilon(3p_{1/2})$ [MeV]
^{210}Po	4.000	0.30	2.455	1.18	0.150	0.00	1.18	1.84	3.14	3.27	3.72
^{208}Po	0.753	0.95	2.455	1.18	0.157	0.00	1.28	1.84	2.82	3.27	3.72
^{206}Po	0.850	1.15	2.421	1.23	0.155	0.00	1.33	1.88	2.89	3.12	3.60
^{204}Po	0.910	1.22	2.317	1.30	0.156	0.00	1.32	1.90	2.78	3.02	3.50
^{202}Po	0.976	1.26	2.117	1.40	0.159	0.00	1.32	1.90	2.78	3.02	3.50
^{200}Po	1.013	1.28	1.950	1.50	0.161	0.00	1.32	1.90	2.78	3.02	3.50

Table 1: Parameters used in the particle-core calculations on the Po isotopes with mass A=210–200. The single-particle energies of the proton orbitals involved in the calculations are given relative to the energy of $1h_{9/2}$. See text for notations.

input	^{A}Pb	194	192	190	188
	HF ($^{A+4}$Po $\rightarrow ^{A}$Pb)	2.8	2.5	1.1	0.44
	β^2 (Pb)	$\frac{0.003}{0.997}$	$\frac{0.005}{0.995}$	$\frac{0.02}{0.98}$	$\frac{0.09}{0.91}$
	^{A}Po	198	196	194	192
	E(0_2^+) [keV]	815	558	229*	303*
	α^2 (Po)	$\frac{0.003}{0.997}$	$\frac{0.01}{0.99}$	$\frac{0.19}{0.81}$	$\frac{0.805}{0.195}$
calc.	δE [keV]	3	7	44	59
	V(0^+)[keV]	52	61	90	120

Table 2: Input for and output information from the two-state mixing calculations involving the ground and the 0_2^+ state in the Po and Pb isotopes. See text for notations. The energies of the 0_2^+ states marked with an asterisk are not known experimentally and were estimated in the present work (see sections 5 and 6.1).

^{A}Po	J^{π}	$E_{exp.}$ [keV]		E_u [keV]		V_{mix} [keV]
		1	2	spherical	intruder	
192	0^+	0.0	–	185	0.0	120
194	0^+	0.0	–	0.0	142	90
	2^+	318	659	542	347	140
	4^+	684.3	1209.4	1115	690	154
	6^+	1145.3	–	(1128–1979)	1128	(27-154)
	8^+	1690	–	–	1646	–
	10^+	2290.6	–	–	2246.6	–
196	0^+	0.0	558(7)	0.0	544	61
	2^+	463	859	561	747	175
	4^+	891	1388	1175	1090	245
	6^+	1390	–	(1528–1796)	1528	(145–245)
	8^+	1939	1974	$\sim$ 1932	($\sim$ 1974)[a]	($\leq$17.5)
	10^+	2591	2778	$\sim$ 2771	$\sim$ 2584 [b]	$\sim$ 0.
198	0^+	0.0	816	0.0	813	51
	2^+	605	1039	622	1016	91
	4^+	1158.5	1483	1276.5	1359	121
	6^+	1717.7	1875.2	1790	1797	79
	8^+	1853.8	2620.7	1850.8	(2315)[c]	–

[a] predicted @2053 keV from intruder band structure. It is not clear that the second observed 8^+ is the intruder state.

[b] predicted @2654 keV from intruder band structure. The two 10^+ states are probably unmixed.

[c] predicted @2315 keV from intruder band structure. The second observed 8^+ state is most probably not of intruder structure.

Table 3: Results of the two-state mixing calculation between the spherical states of spin $0^+ - 8^+$ and the intruder band members with the same spin and parity. The unperturbed positions of both types of states and the mixing matrix elemenst are given. The experimental levels are taken from Ref. [26].

	ϵ MeV	κ MeV	χ_ν	χ_π	$C_{0\nu}$ MeV	$C_{2\nu}$ MeV	$C_{4\nu}$ MeV	$C_{0\pi}$ MeV	$C_{2\pi}$ MeV	$C_{4\pi}$ MeV
N_π=1	0.80	-0.10	0.40	-1.00	0.20	0.10	0.00	0.20	0.10	0.00
N_π=3	0.60	-0.10	0.40	-1.30	0.20	0.10	0.00	0.20	0.10	0.00

Table 4: IBM-2 parameters used in the mixing calculation between the regular ($N_\pi = 1$) and intruder ($N_\pi = 3$) configurations. As required for a best description of the experimental states, Δ was allowed to vary, i.e. Δ=1.5,1.2,0.9,0.7 and 0.55 MeV for A=200–192, respectively. Also α=0.10 and β=0.10 MeV for all Po isotopes. See text for the definition of the parameters.

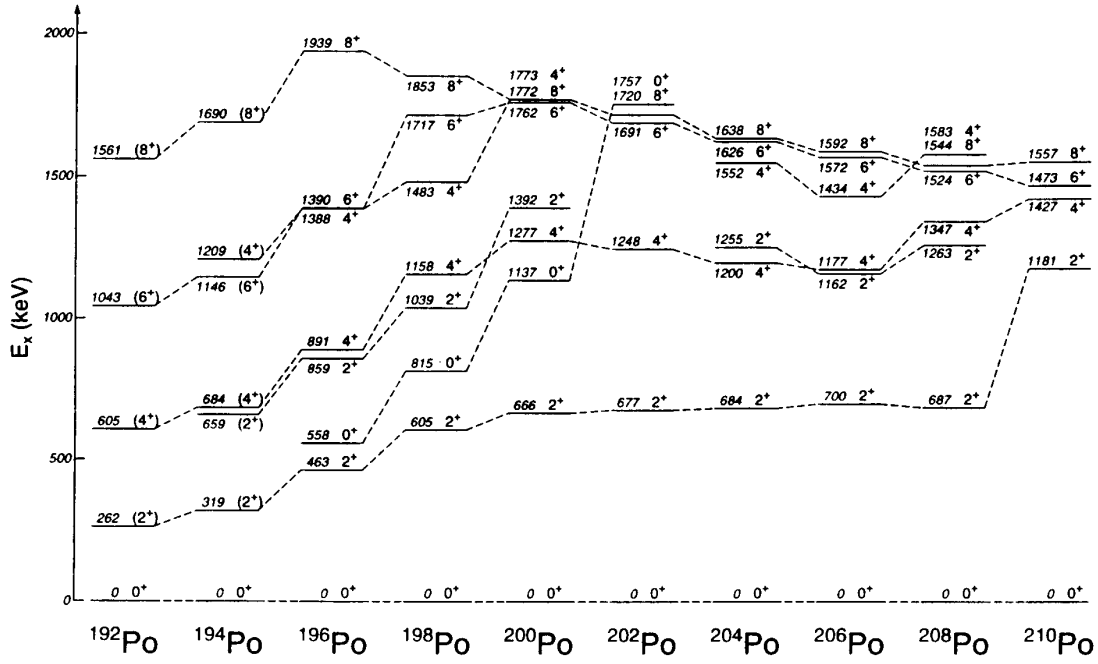

Figure 1: Systematics of the light Po isotopes. Below the shell closure at N=126 with the 'two-proton' nucleus ^{210}Po, a 'regular regime' with smooth variation of the yrast levels is observed down to ^{200}Po. The strong downsloping of the yrast levels in the isotopes below ^{200}Po can be optically associated with the strong lowering in the energy of the first excited 0^+ state. Figure taken from Ref. [24].

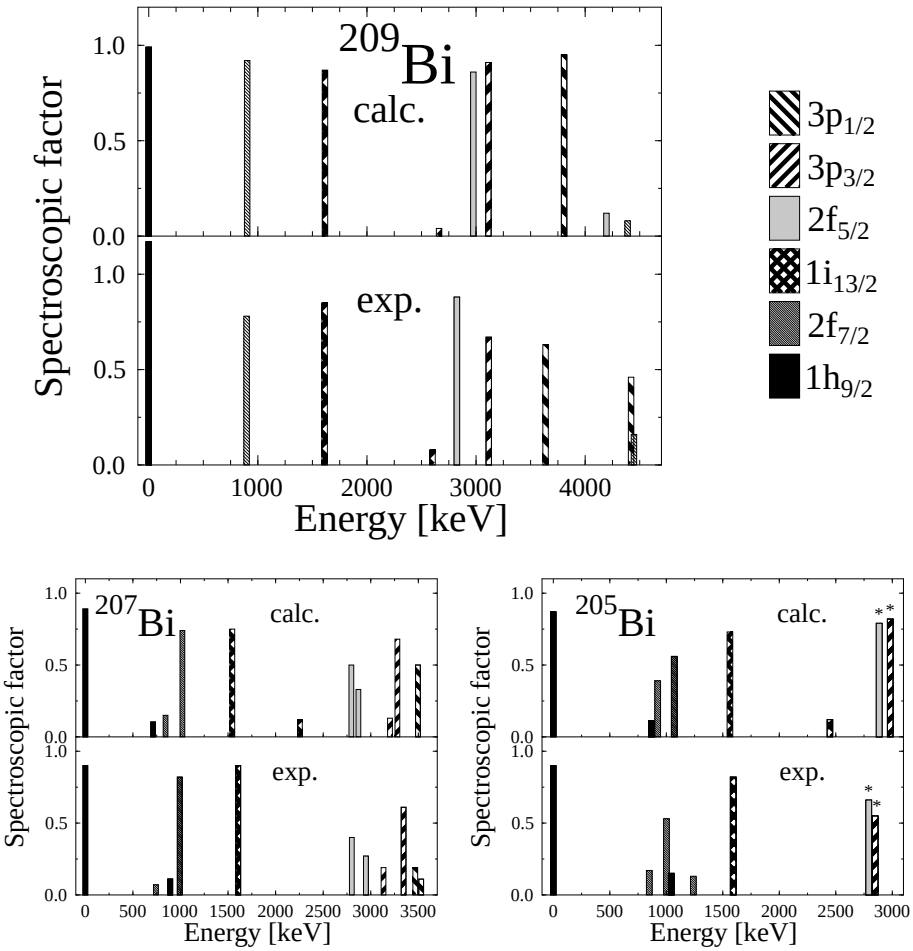

Figure 2: Comparison between the experimental [26] and calculated energies and spectroscopic factors for the states with proton single-particle components in ^{209}Bi, ^{207}Bi and ^{205}Bi. The states belonging to ^{205}Bi, marked with an asterisk, are the centroids of the $\pi 2f_{7/2}$ and $\pi 3p_{3/2}$ single-particle strength distribution.

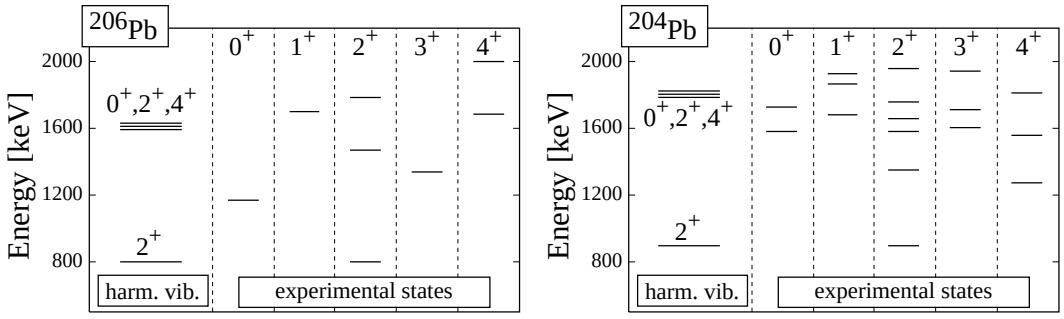

Figure 3: Experimental states of positive parity and spin J=0–4 in ^{206,204}Pb, below E_x=2 MeV. The collective 2_1^+ state and the 'two-phonon' states predicted by a harmonic vibrator picture are shown for comparison. The data are taken from Ref. [26].

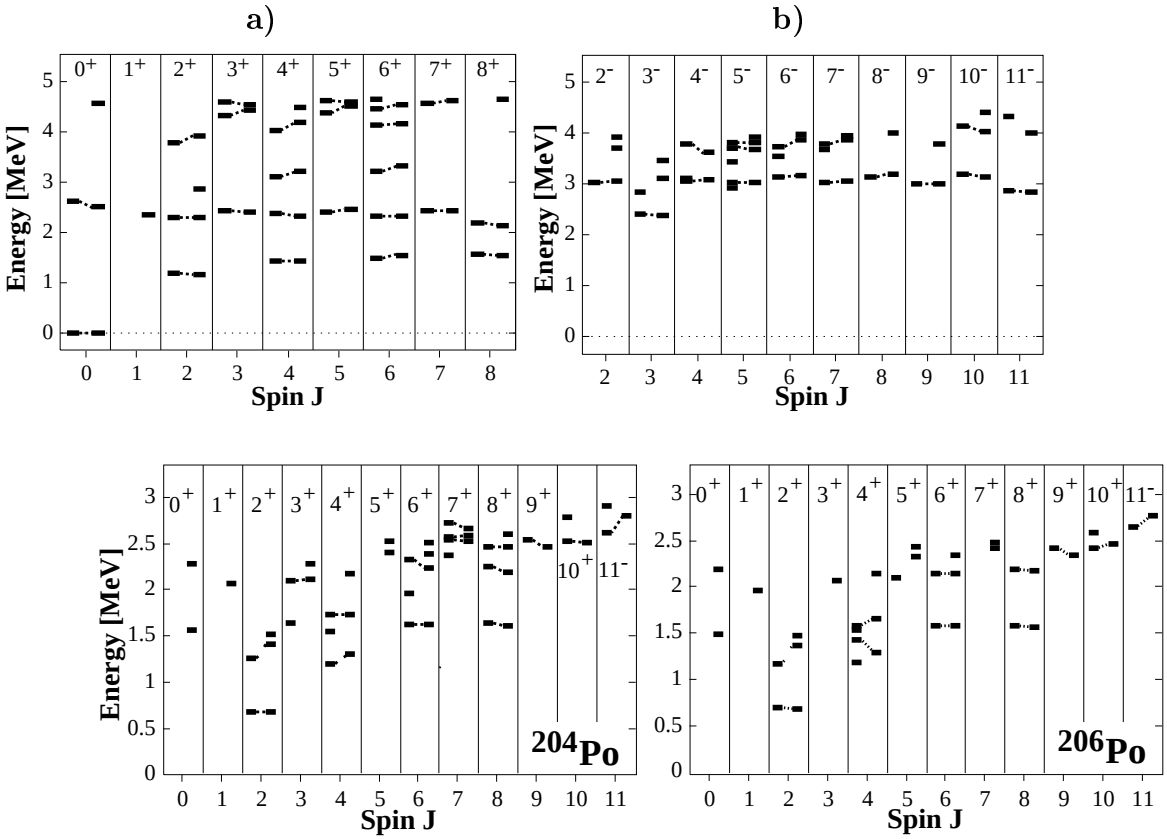

Figure 4: Particle-Core model calculations for the isotopes ^{210}Po (upper part; a) positive parity states and b) negative parity states), ^{206}Po and ^{204}Po (lower part), compared to the experimental states. For each spin and parity value, the experimental states are plotted on the left side and the calculated states on the right side of the figure. Only states below 5 MeV for ^{210}Po and below 3 MeV for the lighter isotopes have been considered. The experimental data are taken from Ref. [26].

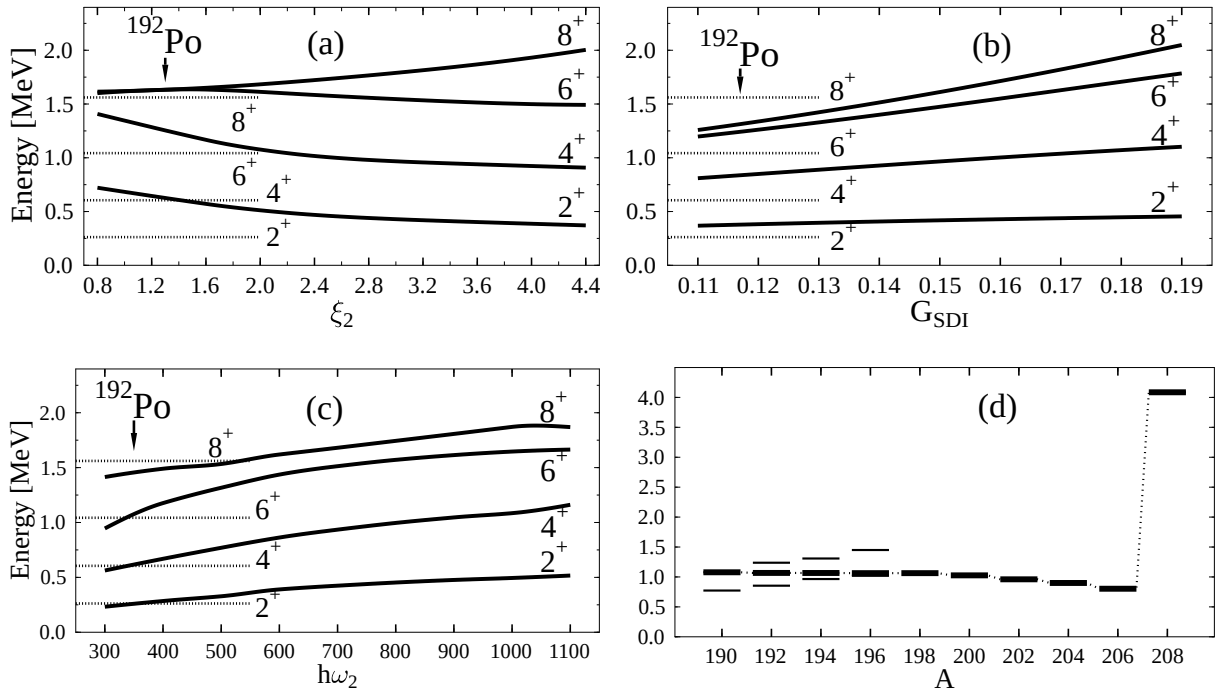

Figure 5: Evolution of the energies of the yrast 0^+–8^+ states as a function of the different model parameters: ξ_2 in part (a), G_{SDI} in part (b) and $\hbar\omega_2$ in part (c). In each case, only the indicated parameter was varied and all the others were kept fixed. The experimental energies of the yrast states in ^{192}Po are shown for comparison on the left side of each figure, plotted with dashed lines. In part (d) we show the evolution with mass number of the energy of the spherical 2^+ state in the Pb isotopes. The energy was corrected for the effects of the mixing between the spherical and intruder 2^+ states, as described in Ref. [42].

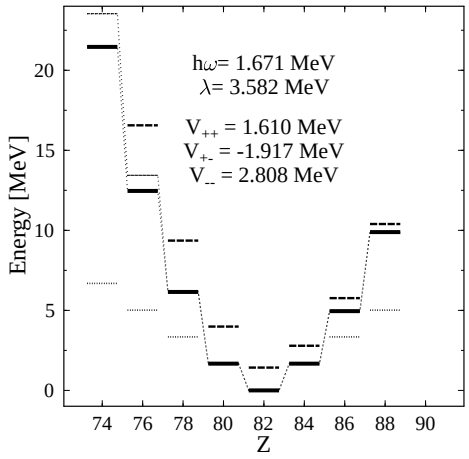

Figure 6: Parameters and predictions of the Pairing Vibration Model for the nuclei around ^{198}Pb (N=116). The experimental energies of the (0,n) and (n,0) states are plotted with thick lines, the harmonic predictions with dotted lines, and the anharmonic ones with dash-dotted line. The predicted (1,n+1) and (n+1,1) 0^+ states are plotted with dashed lines. The notations are explained in the text. The binding energies are taken from Ref. [44].

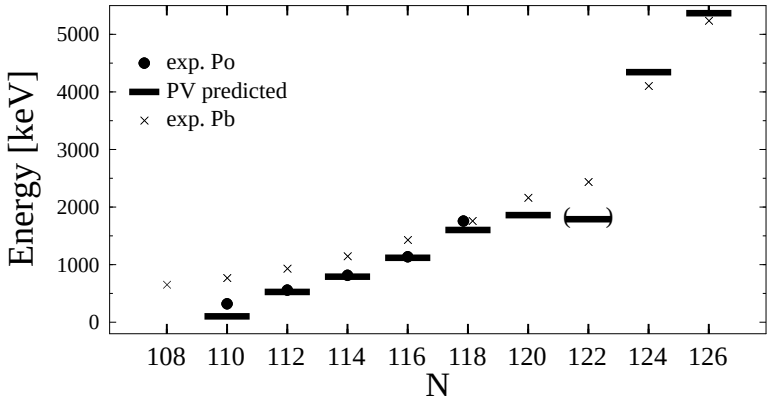

Figure 7: Summary of the predictions of the Pairing Vibration Model for the Po isotopes. The excited 0^+ states with a 4p-2h structure are plotted with lines. The experimental energies of the 0_2^+ states are plotted with dots. The experimental energies of the 0_2^+ states in the Pb isotopes are also shown, plotted with crosses, and were used to deduce part of the model parameters. The predicted 4p-2h state in ^{206}Po (N=122) is only tentative, since the corresponding 0^+ state of 2p-2h character is probably not correctly identified in ^{204}Pb.

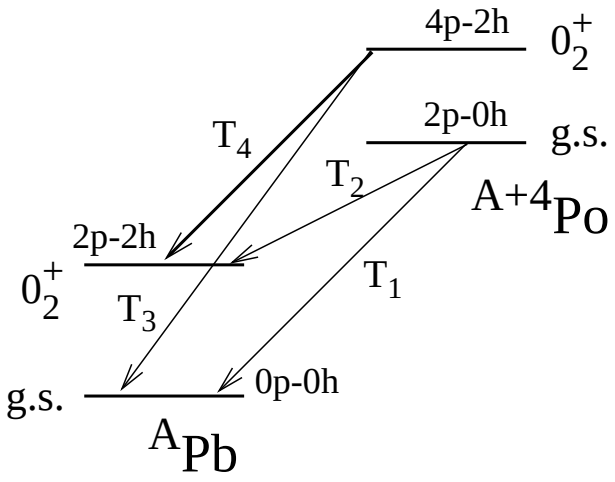

Figure 8: Schematic $\alpha-$decay process from the ground state of a parent nucleus $^{A+4}$Po to the ground state and intruder state of the daughter nucleus ^{A}Pb. The actual ground state and 0_2^+ state in the Po nucleus are supposed to be a mixture of the two configurations shown in the figure, of 2p-0h and 4p-2h character. The same is valid for the daughter nucleus, where the configurations involved are of 0p-0h and 2p-2h character. The matrix elements for the $\alpha-$decay bewteen the four configurations involved are denoted T_1,...,T_4.

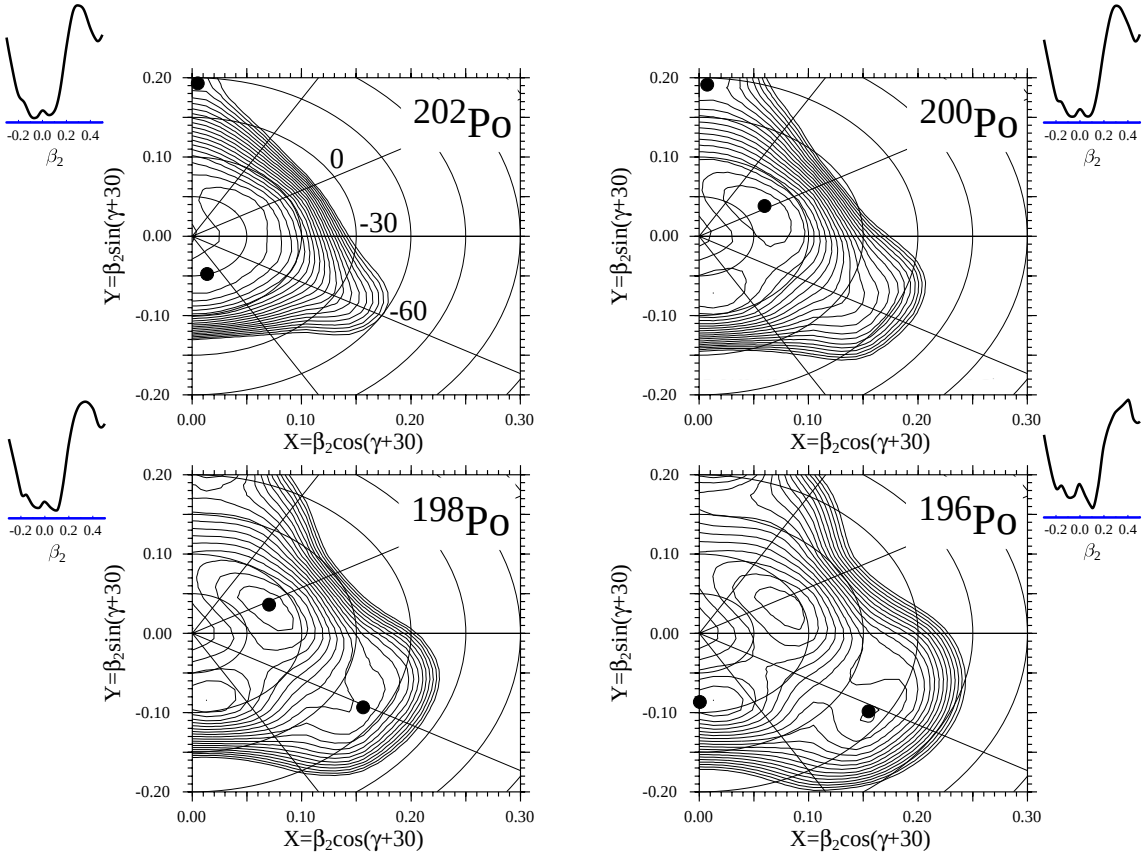

Figure 9: Potential Energy Surface calculations for ^{202,200,198,196}Po. The distance between the contour lines is 100 keV. The minima, marked with dots, correspond to slightly- and well-deformed 0^+ states. The dependence of the total potential energy only on the quadrupole deformation β_2 (study including only axial shapes) is shown for comparison. The shallow structures in the latter potential energy representation correspond to a $\gamma-$soft region in the $\gamma - \beta$ plane and not to real minima.

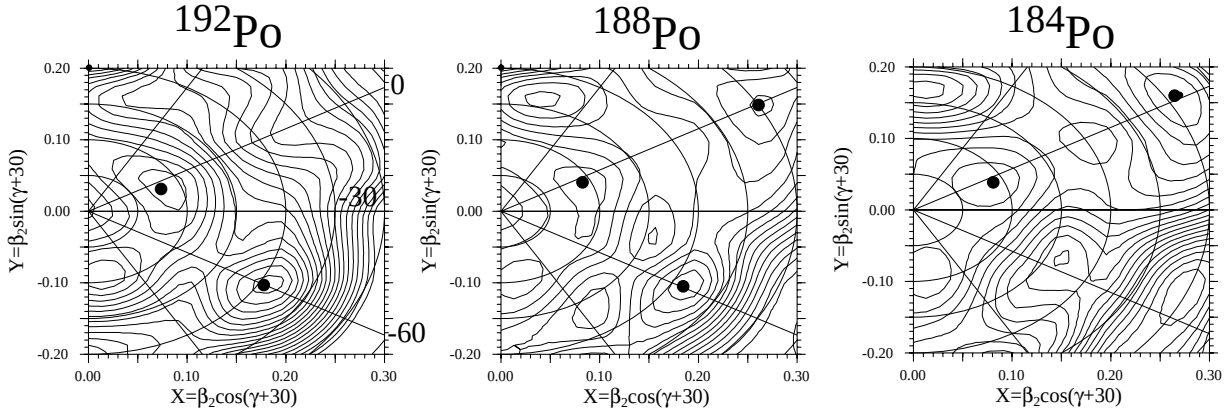

Figure 10: Same as in Fig. 9 for ^{192,188,184}Po. In ^{192}Po the oblate minimum is the most bound one. To be noted is the coexistence of three well-defined minima in ^{188}Po, the nearly spherical, the oblate and a new prolate minimum with β_2=0.30. In ^{184}Po the oblate minimum disappears and two prolate minima coexist, the deepest well-deformed and the higher nearly spherical.

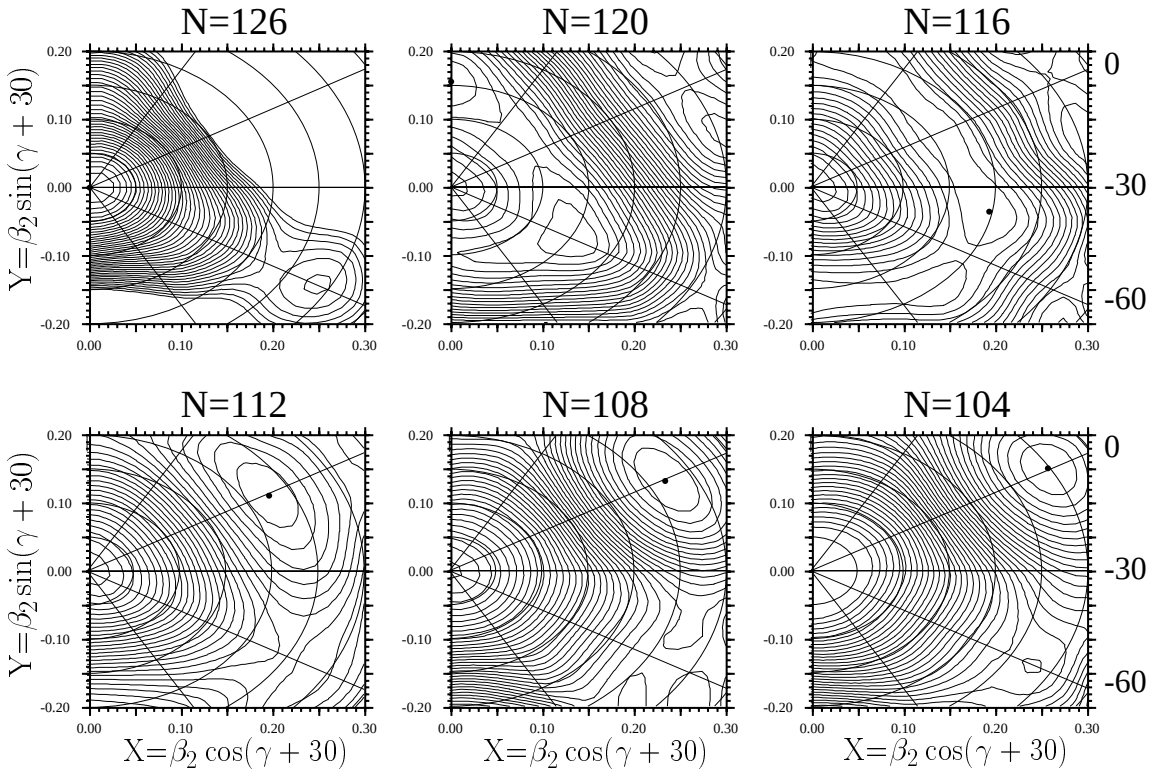

Figure 11: Shell and pairing correction energy for neutrons only. Selected neutron numbers are shown. The distance between the contour lines is 200 keV. The absolute minima are marked with dots.

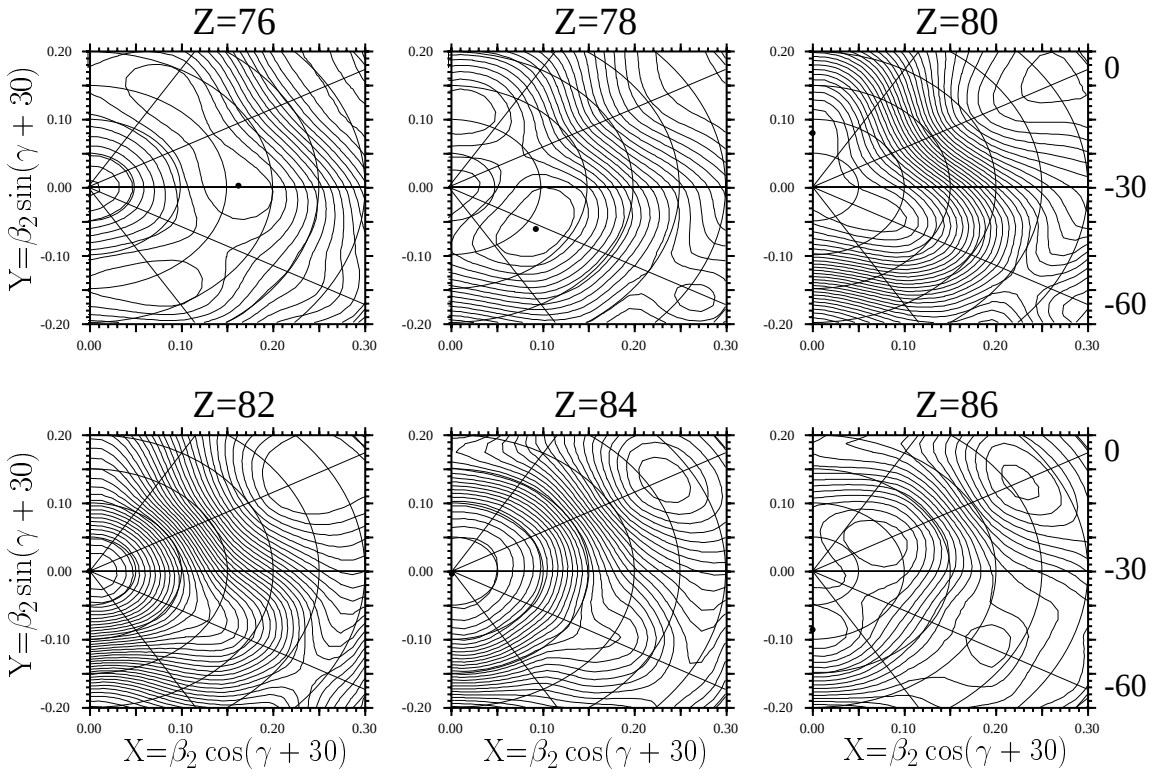

Figure 12: Shell and pairing correction energy for protons only. The proton numbers correspond to the Os, Pt, Hg, Pb, Po and Rn isotopes. The distance between the contour lines is 200 keV. The absolute minima are marked with dots.

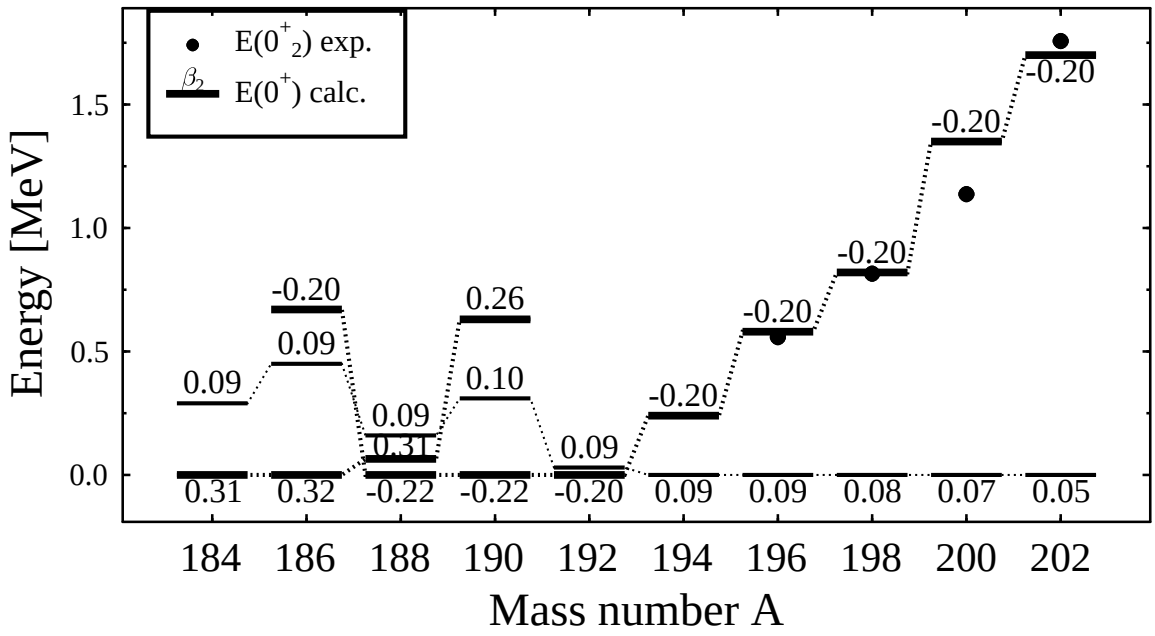

Figure 13: Summary of the predictions of the Potential Energy Surface calculations for $^{202-184}$Po. The oblate configuration is predicted to replace the nearly spherical configuration as the ground state in ^{192}Po, and be afterwards replaced by the strongly deformed prolate configuration in ^{186}Po. No oblate minimum is found in the PES for the nuclei lighter than ^{186}Po. The experimental 0_2^+ states are plotted with dots.

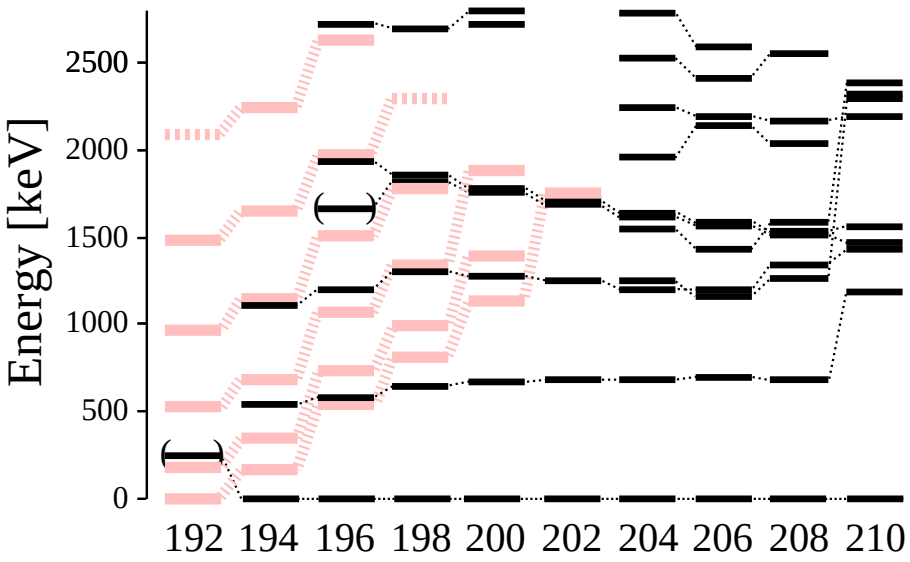

Figure 14: Reconstructed systematics of the Po isotopes, deduced by de-mixing the intruder band and the spherical levels. The regular configurations show little variation across the mass range A=208-194. In contrast, the intruder band (plotted in grey, with thick lines) is lowered strongly in energy when approaching the neutron midshell, in good agreement with the PES calculations and the predictions of the shell-model [1, 2].

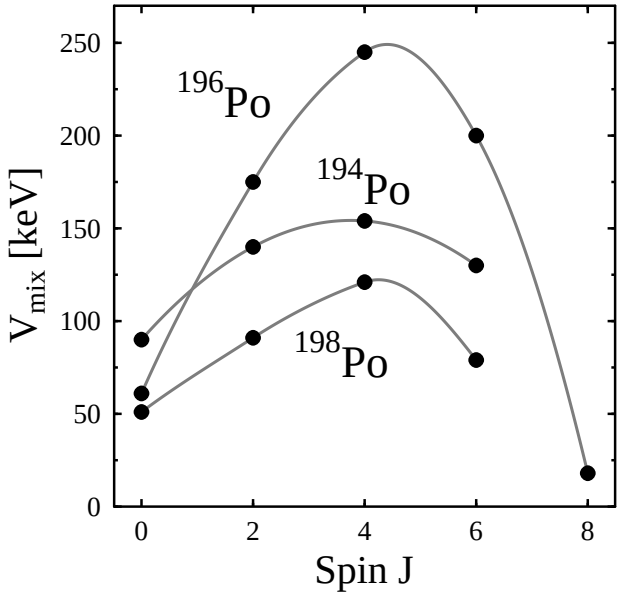

Figure 15: The mixing matrix elements deduced from the two-state mixing calculation show a characteristic J-dependence.

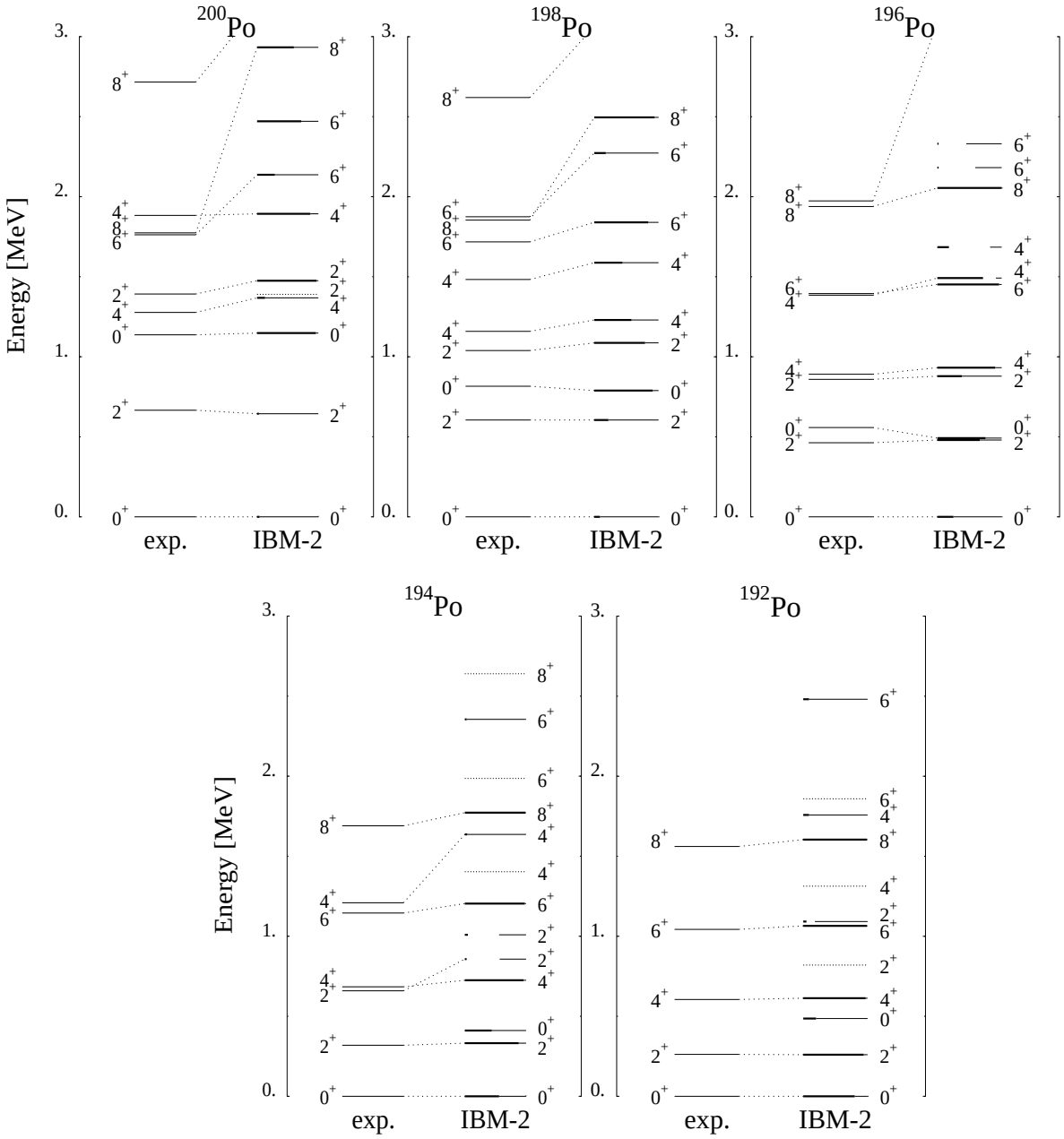

Figure 16: IBM-2 mixing calculation involving a 'regular' and an intruder band for $^{192-200}$Po. The amount of intruder (thick line) and regular (thin line) component is shown for each state. The experimental energies of the states are shown for comparison. The states plotted with dashed lines involve other significant components beside the yrast regular and intruder configurations.

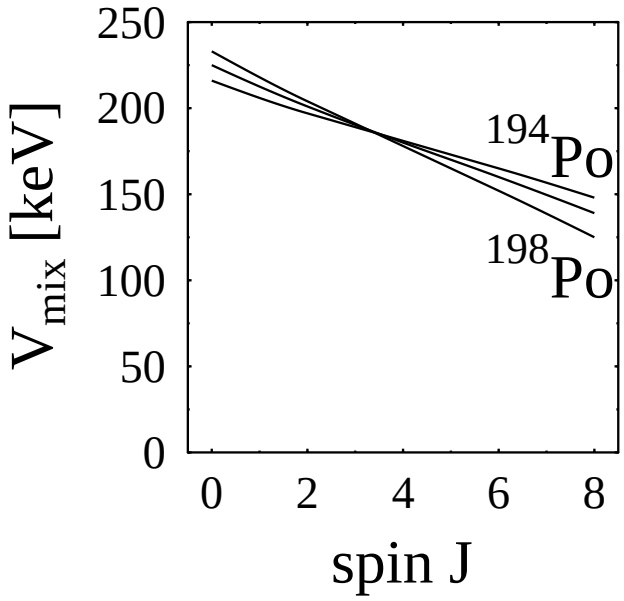

Figure 17: Mixing matrix elements used in the IBM-2 mixing calculation for ^{194}Po, ^{196}Po and ^{198}Po.